Zonotopic set-membership state estimation for switched systems

Sara Ifqir[a, *], Puig Vicenç[b], Ichalal Dalil[c], Ait-Oufroukh Naima[c], Mammar Saïd[c]

[a] CRIStAL, UMR CNRS 9189, Centrale Lille Institut, Villeneuve dAscq, France
[b] Institut de Robòtica i Informàtica Industrial (CSIC-UPC) Carrer Llorens Artigas, 4-6, 08028 Barcelona
[c] IBISC Laboratory, Univ Evry, Paris-Saclay University, Evry, France

Abstract

This paper proposes a new approach for set-membership state estimation of switched discrete-time linear systems subject to bounded disturbances and noises. A zonotopic outer approximation of the state estimation domain is computed and a new criterion is proposed to reduce the size of the zonotope at each sample time. The zonotopic set-membership estimator design for switched systems is provided within the LMI framework. The extension of the proposed scheme to deal with unknown inputs is also presented. An application to vehicle lateral dynamics state estimation is provided. Simulation results demonstrate the effectiveness of the proposed algorithm and highlight its advantages over the existing methods.

1. Introduction

In recent years, switched systems have attracted an increasing interest in the scientific community because of their ability to represent complex and nonlinear behaviours and their applicability to real systems [1]. Switched systems [2,3] is an important class of hybrid

* Corresponding author.
E-mail address: sara.ifqir@centralelille.fr (S. Ifqir).

dynamic systems [4], involving a collection of subsystems and a switching discrete law determining at each time the active subsystem dynamics. The motivation to study this class of systems is mainly twofold. First, several physical and engineering systems can be represented by switched systems, as e.g. chemical processes [5], switching power converters [6], networked control systems [7], automotive and aircraft control [8,9], among other. Second, the design of switched controllers provides a way to overcome the weaknesses of a single controller, which often leads to conservative performances when the system has to operate a wide operating range and parameter variations.

Nowadays, important theoretical results have already been achieved in the literature of switched systems dealing with stability, stabilization and controllability [2,3,10–13], observability, detectability and estimation [14,15]. Since the major problem that is commonly inherent to all dynamic systems is the lack of complete state measurements, the state estimation problem for switched systems has attracted a lot of attention during the last decades [16,17]. The state estimation problem of switched systems was originally studied in [18]. Later, Alessandri and Coletta proposed in [17], a Luenberger-like observer for continuous-time deterministic linear switched systems with known discrete law evolution. In [19], this approach has been extended to the case of unknown discrete modes and a method of discrete and continuous state estimation for linear switched systems has been presented. In [20], an alternative method based on second-order sliding mode observer has been successfully implemented to reconstruct the continuous and discrete states for switched Lagrangian systems. Nevertheless, the state estimation in the presence of model uncertainties represented by unknown (even time-varying) parameters, external disturbances or measurement noises poses great challenges in practical applications. Indeed, in this case, observer design is structurally complicated, since all uncertainties should be either estimated simultaneously or decoupled from the observer equation. In [21–23], the previous approaches are generalized to cover linear and nonlinear switched systems with unknown inputs. In [24,25], classical adaptive observer as well as sliding-mode-based observers techniques have been applied for continuous state reconstruction in the presence of model uncertainty. Besides, robust H_∞ filter design has been widely proposed for switched systems (see [26–29] and references therein). It is noteworthy that, the applicability of each of the aforementioned punctual observers depends heavily on systems uncertainties, especially, if we have to deal with large uncertainties in model parameters, inputs and measurements.

Recently, an attractive alternative approach, known as, bounded-error description, has been proposed [30–35]. In this framework, initiated by Schweppe [36] and Witsenhausen [37], the modeling errors, disturbance, and measurement noise are assumed to be unknown but bounded by a priori known bounds. This hypothesis is motivated by the fact that a lower and upper bounds on model errors and/or measurement is often the only information available in various practical situations. In the literature, several approaches have been proposed to solve the state bounding problem. On the one hand, interval observers based on cooperative systems theory and, on the other hand, set-membership estimators based on set theory. Several types of sets have been used to implement these approaches as ellipsoids [38–40], parallelotopes [41], zonotopes [42–44] and intervals [32,45,46].

This paper proposes a new zonotopic set-membership state estimation approach for uncertain discrete-time switched systems affected by unknown but bounded disturbances and measurement noises. A zonotopic outer approximation of the state estimation domain is computed and a new W-radius minimization criterion is proposed to reduce the size of the zonotope at each sample time. Our methodology offers a good compromise between estimation accuracy and computational complexity. Compared to the relevant existing literature [35,44,47,48], the main contributions of this paper are:

- This paper proposes a new approach for set-membership state estimation of switched discrete-time linear systems subject to bounded disturbances and noises.
- The zonotopic set-membership estimator design for switched systems is provided within the LMI framework;
- Robustness against worst-case disturbances is ensured in a straightforward manner by minimizing directly the effect that the worst-possible input disturbances can have on the resulting W-radius of the state bounding zonotope. Notably, our approach avoids introducing additional constraints and decision variables related to ellipsoid minimization problems used conventionally to minimize the W-radius of the zonotope as done in [49,50]. Simulation results demonstrate the effectiveness of the proposed algorithm and highlight its advantages over the existing methods.
- The developed set-membership state estimation approach is shown to be equivalent to a switched zonotopic observer;
- An extension of the proposed methodology is presented when the system is subject to both bounded uncertainties and unknown inputs;
- Application to vehicle sideslip angle set-membership estimation is presented with and without considering road curvature (unknown input). Experimental evaluation based on real data confirms the efficiency and reliability of the proposed method.

This paper is organized as follows: Section 2 presents the background material regarding zonotopes. In Section 3, zonotopic guaranteed set-membership approach for uncertain switched discrete-time systems is proposed. First, parameterized intersection zonotope is computed by intersecting the measurement state set and the predicted state set. Then, a new optimization methodology subject to LMI constraints is proposed to minimize the radius of the obtained zonotope. Section 4 discusses the equivalence between the proposed set-membership and the zonotopic observer approaches. Section 5 introduces the extension of the proposed observer to the case of dealing with unknown inputs through an Unknown Input Observer (UIO) scheme. Section 6 illustrates the effectiveness of the proposed scheme through an application to vehicle sideslip angle estimation. Finally, conclusions are drawn in Section 7.

2. Preliminaries

In this section, some basic set definitions and operations that will be used along this paper are introduced.

Definition 1. An unitary interval is a vector denoted by $\mathbf{B} = [-1,\ 1]$. An unitary box in $\mathbb{R}^{n_x}$, is a box composed of n_x unitary intervals.

Definition 2 [44]**.** A zonotope of order m in $\mathbb{R}^n$ is the translation by the center $p \in \mathbb{R}^n$ of the image of an unitary hypercube of dimension m in $\mathbb{R}^m$ under a linear transformation $H \in \mathbb{R}^{n\times m}$, the zonotope $\mathbb{X}$ is defined by:

$$\mathbb{X} = \langle p,\ H\rangle = p \oplus H\mathbf{B}^m = \{p + Hz\ :\ z \in \mathbf{B}^m\} \tag{1}$$

Definition 3. The Minkowski sum of two sets $\mathbb{X}_1$ and $\mathbb{X}_2$ is given by $\mathbb{X}_1 \oplus \mathbb{X}_2 = \{x_1 + x_2 : x_1 \in \mathbb{X}_1,\ x_2 \in \mathbb{X}_2\}$.

Property 1. *The Minskowski sum of two zonotopes* $\mathbb{X}_1 = p_1 \oplus H_1\mathbf{B}^{m_1}$ *and* $\mathbb{X}_2 = p_2 \oplus H_2\mathbf{B}^{m_2}$ *is also a zonotope defined by* $\mathbb{X} = \mathbb{X}_1 \oplus \mathbb{X}_2 = (p_1 + p_2) \oplus [H_1\ H_2]\mathbf{B}^{m_1+m_2}$.

Definition 4 (Zonotope interval hull [44]). Consider the zonotope $\mathbb{X} = p \oplus H\mathbf{B}^m$, the smallest interval box that contains this zonotope, i.e. its interval hull denoted by $\square$, is computed by:

$$\square\mathbb{X} = p \oplus rs(H)\mathbf{B}^m \tag{2}$$

where $rs(H)$ is a diagonal matrix such that $rs(H)_{ii} = \sum_{j=1}^{m} |H_{ij}|,\ i = 1, \dots, n$.

Definition 5 (W-radius [51]). Given a zonotope $\mathbb{X} = \langle p, H\rangle \subset \mathbb{R}^n$ and a weighting matrix $W = W^T \succeq 0$, the W-radius of $\mathbb{X}$ is defined by

$$l^W = \max_{x\in\mathbb{X}} \|x - p\|_{2,W}^2 = \max_{z\in\mathbf{B}^q} \|Hz\|_{2,W}^2 \tag{3}$$

where $\|.\|_{2,W}$ is the weighted 2-norm, i.e. $\|Hz\|_{2,W}^2 = z^T H^T W H z$.

Property 2 (Zonotope reduction [51]). *A reduction operator, denoted* $\downarrow_{q,W}$*, allows to reduce the number of generators of a zonotope* $\mathbb{X}$ *to a fixed number* $n \le q < m$*, such that* $\mathbb{X} = \langle p,\ H\rangle \subset \langle p, \downarrow_{q,W} H\rangle$. *A common procedure for implementing the operator* $\downarrow_{q,W}$ *is summarized as follows:*

(1) *Sort the column of segment matrix* $H \in \mathbb{R}^{n\times m}$ *in decreasing weighted vector norm* $\|.\|_W$, $H = [h_1, \dots, h_j, \dots, h_m],\ \|h_j\|_W^2 \ge \|h_{j+1}\|_W^2$;
(2) *Enclose the set* $H_>$ *generated by the* $m - q + n$ *smaller columns into a box (i.e., interval hull):* ***If*** $m \le q$*,* ***then*** $\downarrow_{q,W} H = H$*,* ***Else*** $\downarrow_{q,W} H = [H_>,\ rs(H_<)] \in \mathbb{R}^{n\times q}$, $H_> = [h_1, \dots, h_{q-n}]$, $H_< = [h_{q-n+1}, \dots, h_m]$

where $\|.\|_W$ *is the Frobenius norm and* $rs(H_<)$ *is a diagonal matrix with diagonal elements of* $rs(H_<)_{i,i} = \sum_{j=1}^{m} |H_<|_{i,j},\ i = 1, \dots, n$.

There are other zonotope reduction procedures. A thorough comparison about the existing methods is presented in [52].

3. Set-membership estimator for uncertain switched discrete-time systems

In this work, the following class of stable (or stabilisable) uncertain discrete-time switched systems is considered

$$x_{k+1} = A_{\sigma(k)}x_k + B_{\sigma(k)}u_k + \omega_{\sigma(k)} \tag{4}$$

$$y_k = C_{\sigma(k)}x_k + \upsilon_{\sigma(k)} \tag{5}$$

where $x_k \in \mathbb{R}^{n_x}$, $u_k \in \mathbb{R}^{n_u}$, $y_k \in \mathbb{R}^{n_y}$ denote the vectors of state, input and measurement output, respectively. $\sigma(k) : \mathbb{N}_0 \to I = \{1, 2, \dots, N\}$ is the switching law that determines the discrete mode. It is assumed to be a priori unknown but online available. $A_{\sigma(k)} \in \mathbb{R}^{n_x\times n_x}$, $B_{\sigma(k)} \in \mathbb{R}^{n_x\times n_u}$ and $C_{\sigma(k)} \in \mathbb{R}^{n_y\times n_x}$ are state, input and output matrices. Since no model can exactly represent the state and measurement of the real system considering only the known inputs, the validity of the switched model Eq. (5) includes uncertainty model (modeling errors, disturbances, measurement noise, etc.) with the two additional inputs $\omega_{\sigma(k)} \in \mathbb{R}^{n_x}$ and $\upsilon_{\sigma(k)} \in \mathbb{R}^{n_y}$. Only the knowledge of a bound on their realizations is supposed and no statistical property must be satisfied contrarily to the Kalman filtering approach.

Before we proceed with the detailed set-estimator design, the following assumptions are introduced.

Assumption 1. The initial state is assumed to be unknown but bounded by a zonotope $\mathbb{X}_0 = \langle p_0, H_0\rangle$, where $p_0 \in \mathbb{R}^{n_x}$ and $H_0 \in \mathbb{R}^{n_x \times n_x}$ are the center and segment matrix of this zonotope, respectively.

Assumption 2. $\omega_{\sigma(k)} \in \mathbb{R}^{n_x}$ and $\upsilon_{\sigma(k)} \in \mathbb{R}^{n_y}$ are assumed to be unknown but bounded by zonotopes $\mathbb{W}_{\sigma(k)} = \langle 0, D_{\sigma(k)}\rangle$ and $\mathbb{V}_{\sigma(k)} = \langle 0, F_{\sigma(k)}\rangle$, respectively.

3.1. Parameterized intersection zonotope

Hereafter, a set-membership state estimation approach based on zonotopes for switched discrete-time system Eq. (5) is proposed. This approach is based on *parameterized intersection zonotope* for implementing the measurement consistency test. Before stating the main results, the uncertain state set, measurement state set and exact uncertain set are defined as in [35].

Definition 6 (***Uncertain state set***)**.** Given the switched system Eq. (5) with $x_0 \in \mathbb{X}_0 = \langle p_0, H_0\rangle$, $\omega_{\sigma(k)} \in \mathbb{W}_{\sigma(k)}$, $\forall \sigma(k)$ and for all $k \in \mathbb{N}$, the uncertain state set $\overline{\mathbb{X}}_k$ is defined by

$$\overline{\mathbb{X}}_k = \left\{x \in \mathbb{R}^{n_x} \middle| x \in A_{\sigma(k)}\overline{\mathbb{X}}_{k-1} \oplus B_{\sigma(k)}u_{k-1} \oplus \mathbb{W}_{\sigma(k)}\right\} \tag{6}$$

Definition 7 (***Measurement state set***)**.** Given the switched system Eq. (5), a measurement output vector y_k and $\upsilon_k \in \mathbb{V}_{\sigma(k)}$, $\forall \sigma(k)$ and for all $k \in \mathbb{N}$, the measurement state set $\mathbb{P}_k$ is defined by

$$\mathbb{P}_k = \left\{x \in \mathbb{R}^{n_x} \middle| C_{\sigma(k)}x_k - y_k = F_{\sigma(k)}s_2, \forall s_2 \in \mathbf{B}^{n_y}\right\} \tag{7}$$

Definition 8 (***Exact uncertain set***)**.** Given the switched system Eq. (5), a measurement output vector y_k, $\omega_{\sigma(k)} \in \mathbb{W}_{\sigma(k)}$, $\upsilon_k \in \mathbb{V}_{\sigma(k)}$, $\forall \sigma(k)$ and for all $k \in \mathbb{N}$, the exact uncertain state set $\mathbb{X}(k)$ is defined by

$$\mathbb{X}_k = \overline{\mathbb{X}}_k \cap \mathbb{P}_k \tag{8}$$

The goal is to compute an approximation $\hat{\mathbb{X}}_k$ of the exact uncertain set $\mathbb{X}_k$ by an outer approximation of the intersection between the uncertain trajectory $\overline{\mathbb{X}}_k$ and the region of the state space that is consistent with the measured output y_k and the initial state set $\mathbb{X}_0$ (see Fig. 1).

Based on the prediction and correction steps (detailed in the algorithm below), the procedure of this technique is similar to that of Kalman filter. While the Kalman filter deals with the average case, the proposed set-membership estimator considers the worst case. Now, let us assume that $x_k \in \mathbb{X}_k \subseteq \hat{\mathbb{X}}_k = \langle \hat{p}_k, \hat{H}_k\rangle$ at time $k \in \mathbb{N}$ that also satisfies $x_0 \in \mathbb{X}_0$ at time $k = 0$. Suppose in addition that a measured output y_k is obtained at time instant k. Under these assumptions, an outer bound of the exact uncertain state set $\mathbb{X}_k$ can be estimated using the Algorithm 1.

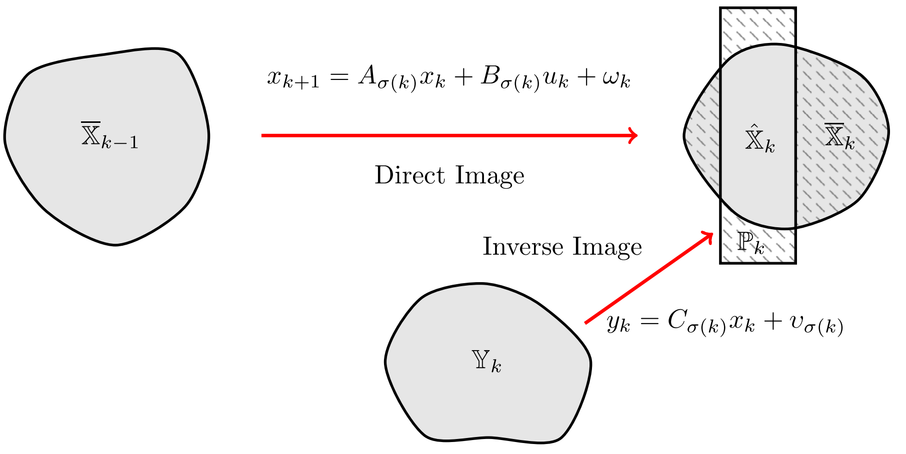

Fig. 1. Set-membership state estimation.

Algorithm 1 Set-membership state estimation.

1. *Prediction step*: Given the switched system Eq. (5), compute the zonotope $\overline{\mathbb{X}}_k$ that bounds the set of predicted states Eq. (6) for the uncertain trajectory of the system using properties of zonotopes in Section 5;
2. *Measurement step*: Parametrize the measurement state set $\mathbb{P}_k$ by using Eq. (7) and taking into account the measurement vector y_k;
3. *Correction step*: To find the state estimation set, compute an outer approximation $\hat{\mathbb{X}}_k$ of the intersection between $\overline{\mathbb{X}}_k$ and $\mathbb{P}_k$

Now let describe how this algorithm can be practically implemented using zonotopes. The key issue is to find a parameterized zonotope $\hat{\mathbb{X}}_k$ that contains the intersection of the two sets $\overline{\mathbb{X}}_k$ and $\mathbb{P}_k$ used in the correction step of the previous algorithm. The zonotope $\hat{\mathbb{X}}_k$ is parameterized with respect to a switched correction matrix $\Lambda_{\sigma(k)} \in \mathbb{R}^{n_x \times n_y}$. The structure of this zonotope is given below.

Proposition 1. *Given the switched system Eq. (5), a measurement output vector y_k, $x_0 \in \mathbb{X}_0$, $\omega_{\sigma(k)} \in \mathbb{W}_{\sigma(k)}$, $\upsilon_k \in \mathbb{V}_{\sigma(k)}$ and $x_{k-1} \in \langle \hat{p}_{k-1}, \hat{H}_{k-1} \rangle \subseteq \langle \hat{p}_{k-1}, \overline{H}_{k-1} \rangle$ with $\overline{H}_{k-1} = \downarrow_{q,W} (\hat{H}_{k-1})$, $\forall \sigma(k)$. Then, for any switched correction matrix $\Lambda_{\sigma(k)} \in \mathbb{R}^{n_x \times n_y}$, we have $x_k \in \left\{ \overline{\mathbb{X}}_k \cap \mathbb{P}_k \right\} \subseteq \hat{\mathbb{X}}_k = \langle \hat{p}_k, \hat{H}_k \rangle$, where*

$$\hat{p}_k = (I_{n_x} - \Lambda_{\sigma(k)} C_{\sigma(k)}) A_{\sigma(k)} \hat{p}_{k-1} + (I_{n_x} - \Lambda_{\sigma(k)} C_{\sigma(k)}) B_{\sigma(k)} u_{k-1} + \Lambda_{\sigma(k)} y_k \tag{9a}$$

$$\hat{H}_k = \left[(I_{n_x} - \Lambda_{\sigma(k)} C_{\sigma(k)}) A_{\sigma(k)} \overline{H}_{k-1}, \quad (I_{n_x} - \Lambda_{\sigma(k)} C_{\sigma(k)}) D_{\sigma(k)}, \quad \Lambda_{\sigma(k)} F_{\sigma(k)} \right] \tag{9b}$$

Proof. . For any $x_k \in \left\{ \hat{\mathbb{X}}_k \cap \mathbb{P}_k \right\}$, it follows that $x_k \in \hat{\mathbb{X}}_k$ and $x_k \in \mathbb{P}_k$. Consider the switched system Eq. (5) with the inclusion $x_{k-1} \in \langle \hat{p}_{k-1}, \hat{H}_{k-1} \rangle \subseteq \langle \hat{p}_{k-1}, \overline{H}_{k-1} \rangle$ and $\omega_{\sigma(k)} \in \mathbb{W}_{\sigma(k)}$, there exists a vector $s_1 \in \mathbf{B}^{q+n_x}$ such that

$$x_k = A_{\sigma(k)}\hat{p}_{k-1} + B_{\sigma(k)}u_{k-1} + \begin{bmatrix} A_{\sigma(k)}\overline{H}_{k-1}, & D_{\sigma(k)} \end{bmatrix} s_1 \tag{10}$$

In addition, from $x_k \in \mathbb{P}_k$, there exists a vector $s_2 \in \mathbf{B}^{n_y}$ such that

$$C_{\sigma(k)}x_k - y_k = F_{\sigma(k)}s_2 \tag{11}$$

Let $\Lambda_{\sigma(k)} \in \mathbb{R}^{n_x \times n_y}$. Adding and subtracting the term $\Lambda_{\sigma(k)}C_{\sigma(k)}\begin{bmatrix} A_{\sigma(k)}\overline{H}_{k-1} & D_{\sigma(k)} \end{bmatrix}s_1$ in Eq. (10), we obtain $\forall \sigma(k)$

$$\begin{aligned} x_k = {} & A_{\sigma(k)}\hat{p}_{k-1} + B_{\sigma(k)}u_{k-1} + \Lambda_{\sigma(k)}C_{\sigma(k)}\begin{bmatrix} A_{\sigma(k)}\overline{H}_{k-1} & D_{\sigma(k)} \end{bmatrix}s_1 \\ & + \begin{bmatrix} (I_{n_x} - \Lambda_{\sigma(k)}C_{\sigma(k)})A_{\sigma(k)}\overline{H}_{k-1} & (I_{n_x} - \Lambda_{\sigma(k)}C_{\sigma(k)})D_{\sigma(k)} \end{bmatrix}s_1 \end{aligned} \tag{12}$$

By substituting x_k in Eq. (11) by Eq. (10), we also have

$$C_{\sigma(k)}\begin{bmatrix} A_{\sigma(k)}\overline{H}_{k-1} & D_{\sigma(k)} \end{bmatrix}s_1 = y_k + F_{\sigma(k)}s_2 - C_{\sigma(k)}(A_{\sigma(k)}\hat{p}_{k-1} + B_{\sigma(k)}u_{k-1}) \tag{13}$$

then, by replacing $C_{\sigma(k)}\begin{bmatrix} A_{\sigma(k)}\overline{H}_{k-1} & D_{\sigma(k)} \end{bmatrix}s_1$ in Eq. (12), it follows that

$$\begin{aligned} x_k = {} & (I_{n_x} - \Lambda_{\sigma(k)}C_{\sigma(k)})A_{\sigma(k)}\hat{p}_{k-1} + (I_{n_x} - \Lambda_{\sigma(k)}C_{\sigma(k)})B_{\sigma(k)}u_{k-1} + \Lambda_{\sigma(k)}y_k \\ & + \begin{bmatrix} (I_{n_x} - \Lambda_{\sigma(k)}C_{\sigma(k)})A_{\sigma(k)}\overline{H}_{k-1} & (I_{n_x} - \Lambda_{\sigma(k)}C_{\sigma(k)})D_{\sigma(k)} & \Lambda_{\sigma(k)}F_{\sigma(k)} \end{bmatrix}\begin{bmatrix} s_1 \\ s_2 \end{bmatrix} \end{aligned} \tag{14}$$

Thus, Eqs. (9a) and (9b) are obtained and the proof is complete. □

3.2. *Optimal switched correction matrix design*

The approach considered in this paper consists in computing a weighting matrix $W_i = W_i^T \succeq 0$ and a correction matrix Λ_i such that for all $i \in I$ and for all $k \geq 0$, the W_i-radius of the zonotopic state estimation set is decreased.

According to Definition 5, the size of the intersection zonotope $\hat{\mathbb{X}}_k$ given by Eq. (9) can be measured by the W_i-radius as follows:

$$\begin{aligned} l_k^W &= \max_{x_k \in \hat{\mathbb{X}}_k} \left\| x_k - \hat{p}_k(\Lambda_{\sigma(k)}) \right\|_{2,W_{\sigma(k)}}^2 \\ &= \max_{z \in \mathbf{B}^{(q+n_x+n_y)}} \left\| \hat{H}_k(\Lambda_{\sigma(k)})z \right\|_{2,W_{\sigma(k)}}^2 \\ &= \max_{z \in \mathbf{B}^{(q+n_x+n_y)}} z^T \hat{H}_k^T(\Lambda_{\sigma(k)})W_{\sigma(k)}\hat{H}_k(\Lambda_{\sigma(k)})z \end{aligned} \tag{15}$$

where $W_{\sigma(k)} = W_i$, $\forall i \in I$ is the weighting matrix of appropriate dimensions for the ith subsystem. As stated above, a suitable design of the correction matrix $\Lambda_{\sigma(k)}$ is required to minimize the effects of uncertainties and guarantee that the size of the intersection zonotope is not increasing. Then, if there exists a scalars $\alpha_{\sigma(k)}$ and $\gamma_{\sigma(k)}$ associated with each subsystem $\sigma(k) = i$ such that

$$\Delta_{k-1}^{l_W} \leq -\alpha_{\sigma(k)}l_{k-1}^W + \gamma_{\sigma(k)}\epsilon_{\sigma(k)} \tag{16}$$

where $\Delta_{k-1}^{l_W} = l_k^W - l_{k-1}^W$ and $\epsilon_{\sigma(k)}$ is a positive switched constant that represents the maximum influence of disturbances and measurement noises as follows:

$$\epsilon_{\sigma(k)} = \max_{b_1 \in \mathbf{B}^{n_x}} \left\| D_{\sigma(k)}b_1 \right\|_2^2 + \max_{b_2 \in \mathbf{B}^{n_y}} \left\| F_{\sigma(k)}b_2 \right\|_2^2 \tag{17}$$

then, the size of $\hat{\mathbb{X}}_k$ is decreasing. If Eq. (16) holds, then for time instant $k \to \infty$, this expression is equivalent for all $i \in I$ to

$$l_\infty^W = (1-\alpha_i) l_\infty^W + \gamma_i \epsilon_i \tag{18}$$

it follows that

$$l_\infty^W = \gamma_i \frac{\epsilon_i}{\alpha_i}, \ \forall i \in \{1, \ldots, N\} \tag{19}$$

To minimize the W-radius (i.e l_∞^W), for given α_i and ϵ_i, the attenuation gain γ_i should be minimized $\forall i \in I$. Then, the design of the correction matrix Λ_i associated with each subsystem i involves solving a Multi-Objective Global Minimum Optimization problem with LMIs constraints according to the following theorem.

Theorem 2. *Consider the intersection zonotope $\mathbb{X}_k = \langle \hat{p}_k, \hat{H}_k \rangle$ in (Eq. 9). Inequality Eq. (16) holds if there exists a matrix $Y_i \in \mathbb{R}^{n_x \times n_y}$, a positive definite matrix $W_i \in \mathbb{R}^{n_x \times n_x}$, scalars $\gamma > 0$, $\gamma_i > 0$ for given scalar $\alpha_i \in (0,1)$ that are obtained by solving the following LMI optimization problem*

$$\min_{W_i, Y_i, \gamma_i} \gamma$$

$$\gamma_i \leq \gamma \tag{20a}$$

$$\begin{bmatrix} (\alpha_i - 1)W_i & * & * & * \\ 0 & -\gamma_i D_i^T D_i & * & * \\ 0 & 0 & -\gamma_i F_i^T F_i & * \\ (W_i - Y_i C_i)A_i & (W_i - Y_i C_i)D_i & Y_i F_i & -W_i \end{bmatrix} \prec 0 \tag{20b}$$

$\forall i \in I$, *with* $Y_i = W_i \Lambda_i$.

Proof. Let $z = \begin{bmatrix} \bar{z}^T & s_1^T & s_2^T \end{bmatrix}^T \in \mathbf{B}^{q+n_x+n_y}$ with $\bar{z} \in \mathbf{B}^q$, $s_1 \in \mathbf{B}^{n_x}$ and $s_2 \in \mathbf{B}^{n_y}$, then using Eq. (15) we have

$$\Delta_{k-1}^{l_W} = \max_{z \in \mathbf{B}^{(q+n_x+n_y)}} \left\| \hat{H}_k(\Lambda_{\sigma(k)}) z \right\|_{2, W_{\sigma(k)}}^2 - \max_{\bar{z} \in \mathbf{B}^q} \left\| \overline{H}_{k-1} \bar{z} \right\|_{2, W_{\sigma(k)}}^2 \tag{21}$$

it follows that

$$\begin{aligned} \Delta_{k-1}^{l_W} &= \max_{\bar{z} \in \mathbf{B}^q, \ z \in \mathbf{B}^{(q+n_x+n_y)}} \left(\left\| \hat{H}_k(\Lambda_{\sigma(k)}) z \right\|_{2, W_{\sigma(k)}}^2 - \left\| \overline{H}_{k-1} \bar{z} \right\|_{2, W_{\sigma(k)}}^2 \right) \\ &= \max_{\bar{z} \in \mathbf{B}^q, s_1 \in \mathbf{B}^{n_x}, s_2 \in \mathbf{B}^{n_y}} \left(\begin{bmatrix} \bar{z} \\ s_1 \\ s_2 \end{bmatrix}^T \hat{H}_k^T(\Lambda_{\sigma(k)}) W_{\sigma(k)} \hat{H}_k(\Lambda_{\sigma(k)}) \begin{bmatrix} \bar{z} \\ s_1 \\ s_2 \end{bmatrix} \right. \\ &\quad \left. - \bar{z}^T \overline{H}_{k-1}^T W_{\sigma(k)} \overline{H}_{k-1} \bar{z} \right) \end{aligned} \tag{22}$$

By adding and subtracting the terms $-\gamma_{\sigma(k)}\epsilon_{\sigma(k)}$ and $\max_{\bar{z}\in\mathbf{B}^q} \alpha_{\sigma(k)} \left\|\overline{H}_{k-1}\bar{z}\right\|^2_{2,W_{\sigma(k)}}$, where $\epsilon_{\sigma(k)}$ is given by Eqs. (17), (22) is rewritten as

$$
\begin{aligned}
\Delta^{l_W}_{k-1} = \max_{\bar{z}\in\mathbf{B}^q, s_1\in\mathbf{B}^{n_x}, s_2\in\mathbf{B}^{n_y}} & \left(\begin{bmatrix} \bar{z} \\ s_1 \\ s_2 \end{bmatrix}^T \hat{H}^T_k(\Lambda_{\sigma(k)}) W_{\sigma(k)} \hat{H}_k(\Lambda_{\sigma(k)}) \begin{bmatrix} \bar{z} \\ s_1 \\ s_2 \end{bmatrix} \right. \\
& + \alpha_{\sigma(k)} \bar{z}^T \overline{H}^T_{k-1} W_{\sigma(k)} \overline{H}_{k-1}\bar{z} - \bar{z}^T \overline{H}^T_{k-1} W_{\sigma(k)} \overline{H}_{k-1}\bar{z} - \gamma_{\sigma(k)} s_1^T D^T_{\sigma(k)} D_{\sigma(k)} s_1 \\
& \left. - \gamma_{\sigma(k)} s_2^T F^T_{\sigma(k)} F_{\sigma(k)} s_2 \right) - \max_{\bar{z}\in\mathbf{B}^q} \alpha_{\sigma(k)} \left\|\overline{H}_{k-1}\bar{z}\right\|^2_{2,W_{\sigma(k)}} + \gamma_{\sigma(k)}\epsilon_{\sigma(k)}
\end{aligned} \tag{23}
$$

Substituting Eq. (9b) into Eq. (23), the above inequality can be rewritten as

$$
\begin{aligned}
\Delta^{l_W}_{k-1} = & \max_{\bar{z}\in\mathbf{B}^q, s_1\in\mathbf{B}^{n_x}, s_2\in\mathbf{B}^{n_y}} \left(\begin{bmatrix} \overline{H}_{k-1}\bar{z} \\ s_1 \\ s_2 \end{bmatrix}^T \left(\Theta^T_{\sigma(k)} W_{\sigma(k)} \Theta_{\sigma(k)} + \right.\right. \\
& \left.\left. \begin{bmatrix} (\alpha_{\sigma(k)} - 1) W_{\sigma(k)} & 0 & 0 \\ 0 & -\gamma_{\sigma(k)} D^T_{\sigma(k)} D_{\sigma(k)} & 0 \\ 0 & 0 & -\gamma_{\sigma(k)} F^T_{\sigma(k)} F_{\sigma(k)} \end{bmatrix} \right) \begin{bmatrix} \overline{H}_{k-1}\bar{z} \\ s_1 \\ s_2 \end{bmatrix} \right) \\
& - \max_{\bar{z}\in\mathbf{B}^q} \alpha_{\sigma(k)} \left\|\overline{H}_{k-1}\bar{z}\right\|^2_{2,W_{\sigma(k)}} + \gamma_{\sigma(k)}\epsilon_{\sigma(k)}
\end{aligned} \tag{24}
$$

where $\Theta_{\sigma(k)} = \begin{bmatrix} (I_{n_x} - \Lambda_{\sigma(k)} C_{\sigma(k)}) A_{\sigma(k)} \\ (I_{n_x} - \Lambda_{\sigma(k)} C_{\sigma(k)}) D_{\sigma(k)} \\ (I_{n_x} - \Lambda_{\sigma(k)} C_{\sigma(k)}) \Lambda_{\sigma(k)} F_{\sigma(k)} \end{bmatrix}^T$. If the following inequality holds $\forall i \in I$

$$
\Theta^T_i W_i \Theta_i + \begin{bmatrix} (\alpha_i - 1) W_i & 0 & 0 \\ 0 & -\gamma_i D^T_i D_i & 0 \\ 0 & 0 & -\gamma_i F^T_i F_i \end{bmatrix} \prec 0 \tag{25}
$$

which is equivalent by means of the application of the Schur complement to Eq. (20b), then, it follows from Eq. (24) that

$$
\Delta^{l_W}_{k-1} \leq -\alpha_i l^W_{k-1} + \gamma_i \epsilon_i, \quad \forall i \in I \tag{26}
$$

Hence, by minimizing the gain γ_i, $\forall i \in I$, the intersection zonotope $\hat{\mathbb{X}}_{k+1}$ can be made as tight as possible. In order to solve this multi-objective optimization problem, one objective scalar γ is minimized while the others are transformed into constraints $\gamma_i \leq \gamma$. This completes the proof of Theorem 2. □

Remark 1. Note that the order of the zonotopes grows with both operations Eqs. (9a) and (9b), increasing the computational and storage requirements. In zonotope-based set-membership state estimation, it is a common practice to iteratively reduce the zonotope order such that it remains upper bounded [51]. When reduction operations take place, the prediction sets in (9) are computed using the reduced order zonotope $\overline{H}_{k-1} = \downarrow_{q,W}(\hat{H}_{k-1})$. Different methods for reducing the order of a zonotope are reviewed in .

3.3. Comparison with existing LMI methods for set-membership estimation

To compare the proposed approach with the existing ones, a straightforward extension of the classical results of zonotopic state estimation [44] to the class of switched system Eq. (5) is presented. Note that, as in the previous sections, a similar two-step procedure (prediction and correction) is applied. Then, according to ([44], Chapter 3) the decreasing condition of the W-radius Eq. (15) can be expressed in the case of switched system as follows:

$$l_k^W \le \tilde{\alpha}_{\sigma(k)} l_{k-1}^W + \epsilon_{\sigma(k)} \tag{27}$$

where $\tilde{\alpha}_{\sigma(k)} \in (0, 1)$ and $\epsilon_{\sigma(k)} = \max_{b_1 \in \mathbf{B}^{n_x}} \left\| D_1 b_1 \right\|_2^2 + \max_{b_2 \in \mathbf{B}^{n_y}} \left\| F_1 b_2 \right\|_2^2$. As $\mathbb{W}_1$ and $\mathbb{V}_1$ are convex sets and the 2-norm is a convex function, the constant $\epsilon_{\sigma(k)}$ can be easily deduced. Subsequently, when k goes to infinity, the condition Eq. (27) is written as $l_\infty^W = \tilde{\alpha}_i l_\infty^W + \epsilon_i$, $\forall i \in I$, leading to

$$l_\infty^W = \frac{\epsilon_i}{1 - \tilde{\alpha}_i}, \quad \forall i \in \{1, \dots, N\} \tag{28}$$

Consider the ith ellipsoid $= \{x : x^T \tilde{W}_i x \le \frac{\epsilon_i}{1-\tilde{\alpha}_i}\}$ which is normalized as follows: $\mathcal{E}_i = \{x : x^T \frac{(1-\tilde{\alpha}_i)\tilde{W}_i}{\epsilon_i} x \le 1\}$. This ellipsoid is related to the $\tilde{W}_i$-Radius of the guaranteed zonotopic state estimation at infinity. Thus, the minimum $\tilde{W}_i$-radius, i.e. l_∞^W, of the zonotope $\hat{\mathbb{X}}_k$ can be obtained by finding the ellipsoid $\mathcal{E}_i$, $\forall i \in I$ of the smallest diameter. This leads to solving the following optimization problem [44]:

$$\max_{\tau_i,\, \tilde{\alpha}_i,\, \tilde{W}_i,\, \tilde{Y}_i} \tau$$

subject to

$$\tau_i \ge \tau \tag{29a}$$

$$\frac{(1-\tilde{\alpha}_i)\tilde{W}_i}{\epsilon_i} \succeq \tau_i I_{n_x} \tag{29b}$$

$$\begin{bmatrix} \tilde{\alpha}_i \tilde{W}_i & * & * & * \\ 0 & D_i^T D_i & * & * \\ 0 & 0 & F_i^T F_i & * \\ \tilde{W}_i A_i - \tilde{Y}_i C_i A_i & \tilde{W}_i D_i - \tilde{Y}_i C_i D_i & \tilde{Y}_i F_i & \tilde{W}_i \end{bmatrix} \succeq 0 \tag{29c}$$

The decision variables are $\tilde{\alpha}_i \in (0, 1)$, τ, $\tau_i > 0$, $\tilde{W}_i = \tilde{W}_i^T \succ 0$, $\tilde{W}_i \in \mathbb{R}^{n_x \times n_x}$ and $\tilde{Y}_i = \tilde{W}_i \tilde{\Lambda}_i \in \mathbb{R}^{n_x \times n_y}$. The BMI optimization problem Eq. (29) is solved by using a search loop on $\tilde{\alpha}_i$ leading to an LMI problem.

In comparison with the optimization problem Eq. (29), Theorem 2 gives a new formulation of robust guaranteed state estimation with guaranteed cost, i.e. γ_i. If for the switched system Eq. (5), Theorem 2 provides feasible solution for W_i and Y_i such that the objective function γ_i attains its minimum value. Then, the resulting zonotope $\mathbb{X}_k$ admits a W_i-radius upper-bounded by

$$l_\infty^W = \gamma_i \frac{\epsilon_i}{\alpha_i}, \quad \forall i \in I \tag{30}$$

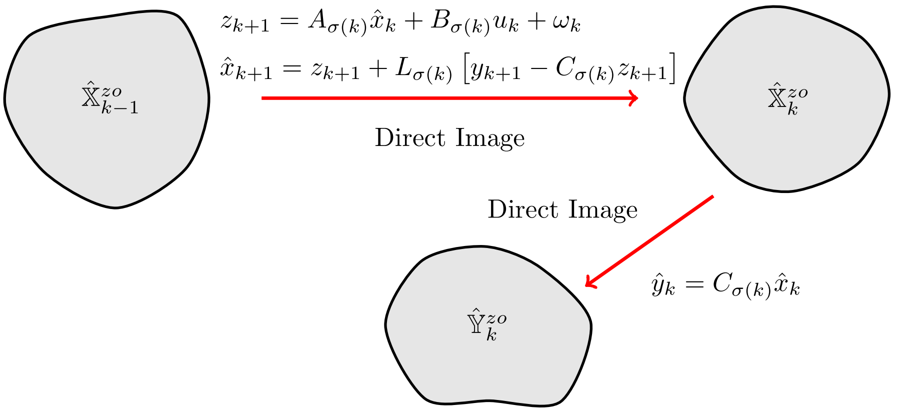

Fig. 2. Zonotopic observer approach.

It should be noticed that the term γ_i, which has no counterpart in the classical zonotopic set-membership estimation theory [44], plays an important role in making the proposed criterion Eq. (30) less conservative than the existing one Eq. (28). The scalar parameter γ_i in Theorem 2 can be appropriately tuned to reduce the adverse effect of disturbance upper bound ϵ_i (i.e. worst case) on the W_i-radius Eq. (26). Accordingly, the main feature of the proposed method is to yield a robust guaranteed estimation procedure, simple to implement, with reduced complexity and less computation time without resorting to ellipsoid minimization problems.

4. Equivalence of the proposed set-membership estimator with a zonotopic observer

In the previous section, a set-membership estimation approach for switched systems based on zonotopes has been proposed. An estimate $\hat{\mathbb{X}}_k$ of the exact consistent state set $\mathbb{X}_k$ has been computed by intersecting the uncertain state set $\overline{\mathbb{X}}_k$ consistent with the model and the one consistent with the measurements $\mathbb{P}_k$ (see Fig. 1). In the sequel, the equivalence of the proposed set-membership estimator and a zonotopic observer for the class of switched system Eq. (5) will be presented. The equivalent switched observer is based on the classical Kalman filter structure [53] where zonotopic sets are used instead of usual Gaussian probability distributions. As illustrated in Fig. 2, the zonotopic observer is a recursive algorithm, that incorporates all the provided information (model and observations) and processes the available measurements to estimate the current state set of the system $\hat{\mathbb{X}}^{zo}_k$. Note that set-membership and interval observer based approaches are commonly thought to be different, although they are already compared to each other in case of LTI systems [54]. In this section, we show that these approaches are actually equivalent, and, produce mathematically identical zonotopes. Comparison of the centers and segments of the obtained zonotopes establish a clear equivalence between the two approaches.

Let us consider the uncertain switched discrete-time system Eq. (5), the structure of the Zonotopic Observer is expressed as

$$z_k = A_{\sigma(k)}\hat{x}_{k-1} + B_{\sigma(k)}u_{k-1} \tag{31a}$$

$$\hat{x}_k = z_k + L_{\sigma(k)}\big[y_k - C_{\sigma(k)}z_k\big] \tag{31b}$$

where $z_k \in \mathbb{R}^{n_x}$ is the apriori estimate of x_k based only on the model and $\hat{x}_k \in \mathbb{R}^{n_x}$ is the posterior estimate of x_k considering both the model and the measurements. $L_{\sigma(k)} \in \mathbb{R}^{n_x \times n_y}$ is the gain matrix to be designed.

The following theorem presents the time evolution of the state zonotopic sets.

Theorem 3. *Given the switched system Eq. (5), measured output y_k, $x_0 \in \mathbb{X}_0$, $\omega_{\sigma(k)} \in \mathcal{W}_{\sigma(k)}$, $\upsilon_k \in \mathcal{V}_{\sigma(k)}$, $\forall \sigma(k)$, $x_{k-1} \in \langle \hat{p}_{k-1}^{zo}, \hat{H}_{k-1}^{zo} \rangle \subseteq \langle \hat{p}_{k-1}^{zo}, \overline{H}_{k-1}^{zo} \rangle$ with $\overline{H}_{k-1}^{zo} = \downarrow_{q,W} (\hat{H}_{k-1}^{zo})$ and a switched gain matrix $L_{\sigma(k)} \in \mathbb{R}^{n_x \times n_y}$. The zonotope bounding uncertain states can be recursively defined by $x_k \in \hat{\mathbb{X}}_k^{zo} = \langle \hat{p}_k^{zo}, \hat{H}_k^{zo} \rangle$, where*

$$\hat{p}_k^{zo} = (I_{n_x} - L_{\sigma(k)} C_{\sigma(k)}) A_{\sigma(k)} \hat{p}_{k-1}^{zo} + (I_{n_x} - L_{\sigma(k)} C_{\sigma(k)}) B_{\sigma(k)} u_k + L_{\sigma(k)} y_k \tag{32a}$$

$$\hat{H}_k^{zo} = \left[(I_{n_x} - L_{\sigma(k)} C_{\sigma(k)}) A_{\sigma(k)} \overline{H}_{k-1}^{zo}, \quad (I_{n_x} - L_{\sigma(k)} C_{\sigma(k)}) D_{\sigma(k)}, \quad L_{\sigma(k)} F_{\sigma(k)} \right] \tag{32b}$$

Proof. Let $e_k = x_k - \hat{x}_k$ be the state estimation error. From Eq. (31), we have

$$\hat{x}_k = (I_{n_x} - L_{\sigma(k)} C_{\sigma(k)}) A_{\sigma(k)} \hat{x}_{k-1} + (I_{n_x} - L_{\sigma(k)} C_{\sigma(k)}) B_{\sigma(k)} u_k + L_{\sigma(k)} y_k \tag{33}$$

Then, the dynamics estimation error can be expressed as

$$\begin{aligned} e_k &= x_k - (I_{n_x} - L_{\sigma(k)} C_{\sigma(k)}) A_{\sigma(k)} \hat{x}_{k-1} - (I_{n_x} - L_{\sigma(k)} C_{\sigma(k)}) B_{\sigma(k)} u_k \\ &\quad - L_{\sigma(k)} C_{\sigma(k)} x_k - L_{\sigma(k)} \upsilon_{\sigma(k)} \\ &= (I_{n_x} - L_{\sigma(k)} C_{\sigma(k)}) x_k - (I_{n_x} - L_{\sigma(k)} C_{\sigma(k)}) A_{\sigma(k)} \hat{x}_{k-1} \\ &\quad - (I_{n_x} - L_{\sigma(k)} C_{\sigma(k)}) B_{\sigma(k)} u_k - L_{\sigma(k)} \upsilon_{\sigma(k)} \\ &= (I_{n_x} - L_{\sigma(k)} C_{\sigma(k)}) A_{\sigma(k)} e_{k-1} + (I_{n_x} - L_{\sigma(k)} C_{\sigma(k)}) \omega_{\sigma(k)} - L_{\sigma(k)} v_{\sigma(k)} \end{aligned} \tag{34}$$

From Eqs. (33) and (34), the uncertain system state x_k is given by

$$\begin{aligned} x_k &= e_k + \hat{x}_k \\ &= (I_{n_x} - L_{\sigma(k)} C_{\sigma(k)}) A_{\sigma(k)} e_{k-1} + (I_{n_x} - L_{\sigma(k)} C_{\sigma(k)}) \omega_{\sigma(k)} - L_{\sigma(k)} v_{\sigma(k)} \\ &\quad + (I_{n_x} - L_{\sigma(k)} C_{\sigma(k)}) A_{\sigma(k)} \hat{x}_{k-1} + (I_{n_x} - L_{\sigma(k)} C_{\sigma(k)}) B_{\sigma(k)} u_{k-1} + L_{\sigma(k)} y_k \\ &= (I_{n_x} - L_{\sigma(k)} C_{\sigma(k)}) A_{\sigma(k)} x_{k-1} + (I_{n_x} - L_{\sigma(k)} C_{\sigma(k)}) \omega_{\sigma(k)} - L_{\sigma(k)} v_{\sigma(k)} \\ &\quad + (I_{n_x} - L_{\sigma(k)} C_{\sigma(k)}) B_{\sigma(k)} u_k + L_{\sigma(k)} y_k \end{aligned} \tag{35}$$

Considering the uncertain system state $x_{k-1} \in \mathbb{X}_{k-1}^{zo} = \langle \hat{p}_{k-1}^{zo}, \hat{H}_{k-1}^{zo} \rangle \subseteq \langle \hat{p}_{k-1}^{zo}, \overline{H}_{k-1}^{zo} \rangle$ as prior, the uncertain state at time instant k can also be bounded by the zonotope $\mathbb{X}_k^{zo} = \langle \hat{p}_k^{zo}, \hat{H}_k^{zo} \rangle$ that is defined as follows:

$$\begin{aligned} x_{k+1} &= (I_{n_x} - L_{\sigma(k)} C_{\sigma(k)}) A_{\sigma(k)} \hat{p}_k + (I_{n_x} - L_{\sigma(k)} C_{\sigma(k)}) B_{\sigma(k)} u_k + L_{\sigma(k)} y_{k+1} \\ &\qquad + \left[(I_{n_x} - L_{\sigma(k)} C_{\sigma(k)}) A_{\sigma(k)} \hat{H}_k, \quad (I_{n_x} - L_{\sigma(k)} C_{\sigma(k)}) D_{\sigma(k)}, \quad L_{\sigma(k)} F_{\sigma(k)} \right] \begin{bmatrix} s_1 \\ s_2 \\ -s_3 \end{bmatrix} \end{aligned} \tag{36}$$

where $s_1 \in \mathbf{B}^q$, $s_2 \in \mathbf{B}^{n_\omega}$ and $s_3 \in \mathbf{B}^{n_\upsilon}$. Thus, Eqs. (32a) and (32b) are obtained and the proof is complete. □

Remark 2. Recall that, the zonotope reduction operator $\downarrow_{q,W} (.)$ defined in Property 2 is used in order to reduce the computational complexity during the state propagations.

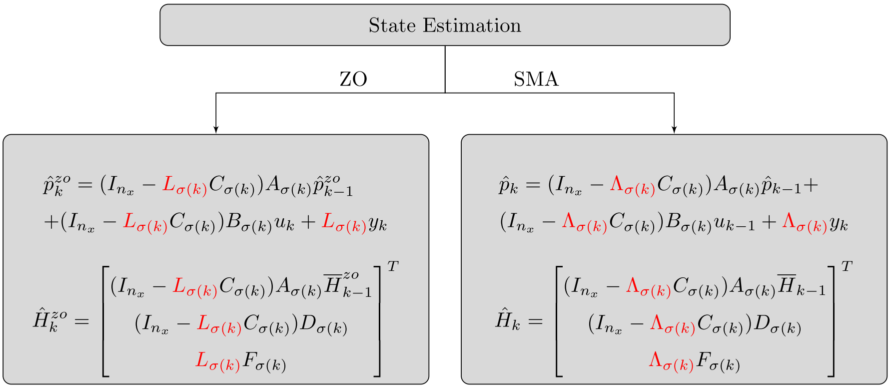

Fig. 3. Zonotopic Observer (ZO) versus Set-Membership Approach (SMA) using zonotopes.

Note that the predicted center and segments Eq. (32) computed using the zonotopic interval-observer approach are similar in structure to those in Eq. (9) provided using the set-membership state estimation approach. As shown in Fig. 3, since the two structures are equivalent, the observer gain $L_{\sigma(k)}$ can be obtained by using the same optimization problem proposed for the set-membership approach in Theorem 2, i.e. to obtain $\Lambda_{\sigma(k)}$.

Corollary 4. *Given the zonotopic observer with the structure defined in Theorem 3, the optimal switched gain matrix $L_{\sigma(k)}$ can be obtained following the same procedure as the one described in Theorem 2.*

This equivalence is illustrated using the case study presented in Section 6.

5. Extension to consider unknown inputs

In this section, we will extend the proposed set-membership state estimation approach for uncertain switched discrete-time systems subject to unknown inputs.

Let us consider again discrete-time switched model Eq. (5) but now including unknown inputs

$$\begin{aligned} x_{k+1} &= A_{\sigma(k)}x_k + B_{\sigma(k)}u_k + E_{\sigma(k)}d_k + \omega_{\sigma(k)} \\ y_k &= C_{\sigma(k)}x_k + \upsilon_{\sigma(k)} \end{aligned} \tag{37}$$

where $x_k \in \mathbb{R}^{n_x}$, $u_k \in \mathbb{R}^{n_u}$, $d_k \in \mathbb{R}^{n_d}$, $y_k \in \mathbb{R}^{n_y}$ denote the state, known and unknown inputs and measurement output vectors, respectively. $A_{\sigma(k)} \in \mathbb{R}^{n_x \times n_x}$, $B_{\sigma(k)} \in \mathbb{R}^{n_x \times n_u}$, $E_{\sigma(k)} \in \mathbb{R}^{n_x \times n_d}$ and $C_{\sigma(k)} \in \mathbb{R}^{n_y \times n_x}$ are state, input, unknown input and output distribution matrices. The switching signal $\sigma(k)$ is a piecewise-constant function, which takes its values in the finite set $I = \{1, \ldots, N\}$, where $N > 1$ is the number of subsystems. $\omega_{\sigma(k)} \in \mathbb{R}^{n_\omega}$ and $\upsilon_{\sigma(k)} \in \mathbb{R}^{n_\upsilon}$ represent the state disturbance and measurement noise vectors, respectively.

Before we proceed with the detailed set-estimator design, the following additional assumptions are considered.

Assumption 3. For the switched system Eq. (37), let us assume that the following rank condition is satisfied $\forall \sigma(k) \in I, \quad k \in \mathbb{N}$:

$$rank(C_{\sigma(k)}E_{\sigma(k)}) = rank(E_{\sigma(k)}) = n_d \tag{38}$$

Thus, there exists a non-empty set of solutions of switched matrices $P_{\sigma(k)}$ and $M_{\sigma(k)}$ satisfying $\forall\sigma(k)$

$$\begin{aligned} P_{\sigma(k)} + M_{\sigma(k)}C_{\sigma(k)} &= I_{n_x} \\ P_{\sigma(k)}E_{\sigma(k)} &= 0 \end{aligned} \tag{39}$$

Remark 3. Assumption 3 means that all the unknown inputs contained in the vector d_k are able to be decoupled by the proposed unknown input set-membership estimator. However, it should be pointed out that, there could be some difficulties to satisfy the rank condition given in Eq. (38). In this case, the design conditions of the traditional unknown input observers can be solved by decoupling a part of unknown inputs included in d_k, and, by rewriting:

$$d_k = \begin{bmatrix} d_k^1 \\ d_k^2 \end{bmatrix} \tag{40}$$

where $d_k^1 \in \mathbb{R}^{n_{d1}}$ denotes the unknown input vector that can be actively decoupled, while $d_k^2 \in \mathbb{R}^{n_{d2}}$ is the remaining number of unknown inputs to be treated as bounded uncertainties. Correspondingly, the matrix $E_{\sigma(k)}$ can be rewritten as

$$E_{\sigma(k)} = \begin{bmatrix} E_{\sigma(k)}^1 & E_{\sigma(k)}^2 \end{bmatrix} \tag{41}$$

where $E_{\sigma(k)}^1 \in \mathbb{R}^{n_x \times n_{d1}}$ and $E_{\sigma(k)}^2 \in \mathbb{R}^{n_x \times n_{d2}}$. As a result, the switched system dynamics Eq. (37) can be further rewritten as

$$\begin{aligned} x_{k+1} &= A_{\sigma(k)}x_k + B_{\sigma(k)}u_k + E_{\sigma(k)}^1 d_k^1 + \omega_{\sigma(k)}^1 \\ y_k &= C_{\sigma(k)}x_k + \upsilon_{\sigma(k)} \end{aligned} \tag{42}$$

with $rank(CE_{\sigma(k)}^1) = rank(E_{\sigma(k)}^1) = n_{d1}$ and $\omega_{\sigma(k)}^1 = \omega_{\sigma(k)} + E_{\sigma(k)}^2 d_k^2$ is assumed to be unknown bounded by a given zonotope (i.e., $\omega_{\sigma(k)}^1 \in \mathbb{W}_{\sigma(k)}^1$). It should be emphasized that the decomposition Eq. (40) can be also used to overcome some limitations of the set-based approaches, namely, when some system disturbances are unknown and difficult or impossible to be bounded in a predefined zonotope. In this case, unbounded disturbances are considered as unknown inputs and are decoupled completely in the switched observer design.

In Section 3, an outer-approximation $\hat{\mathbb{X}}_k$ of the intersection between uncertain trajectory $\overline{\mathbb{X}}_k$ and the region of the state space $\mathbb{P}_k$ which is consistent with the measured output is computed. The outer-approximation is parameterized by the correction matrix $\Lambda_{\sigma(k)}$ using a zonotope-based procedure. In what follows, this approach is extended to the class of systems of the form Eq. (37). For sake of clarity, measurement state set $\mathbb{P}_k$ and exact uncertain set $\mathbb{X}_k$ are defined in the same way as in Definitions Eqs. (7) and (8) while the uncertain state set $\overline{\mathbb{X}}_k$ is redefined below in order to take into account the effect of the unknown input d_k. Subsequently, an outer bound of the exact uncertain state set $\mathbb{X}_k$ is estimated using the same steps as in Algorithm 1. Based on a judicious design methodology, the effect of the unknown inputs is effectively cancelled.

Definition 9 (***Uncertain state set***)**.** Given the switched system Eq. (37) with $x_0 \in \mathbb{X}_0$, $\omega_{\sigma(k)} \in \mathbb{W}_{\sigma(k)}$, $\forall\sigma(k)$ and for all $k \in \mathbb{N}$, the uncertain state set $\overline{\mathbb{X}}_k$ is defined by

$$\overline{\mathbb{X}}_k = \left\{ x \in \mathbb{R}^{n_x} \middle| x \in A_{\sigma(k)}\overline{\mathbb{X}}_{k-1} \oplus B_{\sigma(k)}u_{k-1} \oplus D_{\sigma(k)}\mathbb{W}_{\sigma(k)} \oplus E_{\sigma(k)}d_{k-1} \right\} \tag{43}$$

5.1. Guaranteed state intersection

We now present the set-membership state estimation approach for the uncertain switched discrete-time system Eq. (37). An outer approximation of the exact estimation set $\mathbb{X}_k$ is obtained by intersecting the predicted state $\overline{\mathbb{X}}_k$ and the measurement set $\mathbb{P}_k$. This statement is summarized by means of the following theorem.

Theorem 5. *Given the switched system Eq. (37), a measurement output vector y_k, $x_0 \in \mathbb{X}_0$, $\omega_{\sigma(k)} \in \mathbb{W}_{\sigma(k)}$, $\upsilon_k \in \mathbb{V}_{\sigma(k)}$, $\forall \sigma(k)$, $x_{k-1} \in \langle \hat{p}_{k-1}, \hat{H}_{k-1} \rangle \subseteq \langle \hat{p}_{k-1}, \overline{H}_{k-1} \rangle$ with $\overline{H}_{k-1} = \downarrow_{q,W} (\hat{H}_{k-1})$, $P_{\sigma(k)} \in \mathbb{R}^{n_x \times n_x}$ and $M_{\sigma(k)} \in \mathbb{R}^{n_x \times n_y}$ satisfying Eq. (39). Then, for any switched correction matrix $\Lambda_{\sigma(k)} \in \mathbb{R}^{n_x \times n_y}$, $x_k \in \left\{ \overline{\mathbb{X}}_k \cap \mathbb{P}_k \right\} \subseteq \hat{\mathbb{X}}_k = \langle \hat{p}_k, \hat{H}_k \rangle$, where*

$$\begin{aligned} \hat{p}_k = {} & T_{\sigma(k)} P_{\sigma(k)} A_{\sigma(k)} \hat{p}_{k-1} + T_{\sigma(k)} P_{\sigma(k)} B_{\sigma(k)} u_{k-1} \\ & + (M_{\sigma(k)} + \Lambda_{\sigma(k)} - \Lambda_{\sigma(k)} C_{\sigma(k)} M_{\sigma(k)}) y_k \end{aligned} \tag{44a}$$

$$\hat{H}_k = \left[T_{\sigma(k)} P_{\sigma(k)} A_{\sigma(k)} \overline{H}_{k-1} \quad T_{\sigma(k)} P_{\sigma(k)} D_{\sigma(k)} \quad T_{\sigma(k)} M_{\sigma(k)} F_{\sigma(k)} \quad \Lambda_{\sigma(k)} F_{\sigma(k)} \right] \tag{44b}$$

where $T_{\sigma(k)} = I_{n_x} - \Lambda_{\sigma(k)} C_{\sigma(k)}$.

Proof. For any $x_k \in \left\{ \overline{\mathbb{X}}_k \cap \mathbb{P}_k \right\}$, we know $x_k \in \overline{\mathbb{X}}_k$ and $x_k \in \mathbb{P}_k$. Consider the switched system Eq. (37) with the inclusion $x_{k-1} \in \langle \hat{p}_{k-1}, \hat{H}_{k-1} \rangle \subseteq \langle \hat{p}_{k-1}, \overline{H}_{k-1} \rangle$ and $\omega_{\sigma(k)} \in \mathbb{W}_{\sigma(k)}$, there exists a vector $s_1 \in \mathbf{B}^{q+n_\omega}$ such that

$$x_k = A_{\sigma(k)} \hat{p}_{k-1} + B_{\sigma(k)} u_{k-1} + E_{\sigma(k)} d_{k-1} + \left[A_{\sigma(k)} \overline{H}_{k-1}, \quad D_{\sigma(k)} \right] s_1 \tag{45}$$

Besides, from $x_k \in \mathbb{P}_k$, there exists a vector $s_2 \in \mathbf{B}^{n_\upsilon}$ such that

$$C_{\sigma(k)} x_k - y_k = F_{\sigma(k)} s_2 \tag{46}$$

Considering a pair of switched matrices $P_{\sigma(k)}$ and $M_{\sigma(k)}$ satisfying Eq. (39) $\forall \sigma(k)$, combining Eqs. (45) and (46) leads to

$$\begin{aligned} & (P_{\sigma(k)} + M_{\sigma(k)} C_{\sigma(k)}) x_k = P_{\sigma(k)} A_{\sigma(k)} \hat{p}_{k-1} + P_{\sigma(k)} B_{\sigma(k)} u_{k-1} + P_{\sigma(k)} E_{\sigma(k)} d_{k-1} + \\ & M_{\sigma(k)} y_k + \left[P_{\sigma(k)} A_{\sigma(k)} \overline{H}_{k-1} \quad P_{\sigma(k)} D_{\sigma(k)} \right] s_1 + M_{\sigma(k)} F_{\sigma(k)} s_2 \end{aligned} \tag{47}$$

Set $R_{\sigma(k)} = \left[P_{\sigma(k)} A_{\sigma(k)} \overline{H}_{k-1} \quad P_{\sigma(k)} D_{\sigma(k)} \quad M_{\sigma(k)} F_{\sigma(k)} \right]$ and $s = \left[s_1^T, \quad s_2^T \right]^T$. If the matrix Eq. (39) hold, then Eq. (47) can be simplified as follows

$$x_k = P_{\sigma(k)} A_{\sigma(k)} \hat{p}_{k-1} + P_{\sigma(k)} B_{\sigma(k)} u_{k-1} + M_{\sigma(k)} y_k + R_{\sigma(k)} s \tag{48}$$

Let $\Lambda_{\sigma(k)} \in \mathbb{R}^{n_x \times n_x}$, by adding and substituting a correction term $\Lambda_{\sigma(k)} C_{\sigma(k)} R_{\sigma(k)} s$ in Eq. (48), we obtain $\forall \sigma(k)$

$$\begin{aligned} & x_k = P_{\sigma(k)} A_{\sigma(k)} \hat{p}_{k-1} + P_{\sigma(k)} B_{\sigma(k)} u_{k-1} + M_{\sigma(k)} y_k \\ & + \Lambda_{\sigma(k)} C_{\sigma(k)} R_{\sigma(k)} s + (I_{n_x} - \Lambda_{\sigma(k)} C_{\sigma(k)}) R_{\sigma(k)} s \end{aligned} \tag{49}$$

By multiplying in both side of Eq. (49) by $C_{\sigma(k)}$ and substituting $C_{\sigma(k)} x_k$ in Eq. (49) by Eq. (46), we have

$$\begin{aligned} C_{\sigma(k)} R_{\sigma(k)} s = {} & y_k - C_{\sigma(k)} M_{\sigma(k)} y_k - C_{\sigma(k)} P_{\sigma(k)} A_{\sigma(k)} \hat{p}_{k-1} \\ & - C_{\sigma(k)} P_{\sigma(k)} B_{\sigma(k)} u_{k-1} + F_{\sigma(k)} s_1 \end{aligned} \tag{50}$$

then, by replacing $C_{\sigma(k)}R_{\sigma(k)}s$ in Eq. (49) by Eq. (50), it follows that

$$
\begin{aligned}
x_k = &(I_{n_x} - \Lambda_{\sigma(k)}C_{\sigma(k)})P_{\sigma(k)}A_{\sigma(k)}\hat{p}_{k-1} + (I_{n_x} - \Lambda_{\sigma(k)}C_{\sigma(k)})P_{\sigma(k)}B_{\sigma(k)}u_{k-1} \\
&+ (M_{\sigma(k)} + \Lambda_{\sigma(k)} - \Lambda_{\sigma(k)}C_{\sigma(k)}M_{\sigma(k)})y_k \\
&+ \left[(I_{n_x} - \Lambda_{\sigma(k)}C_{\sigma(k)})R_{\sigma(k)}, \quad \Lambda_{\sigma(k)}F_{\sigma(k)}\right]\begin{bmatrix} s \\ s_1 \end{bmatrix}
\end{aligned} \tag{51}
$$

Thus, by using the above definition of $R_{\sigma(k)}$ and by letting $T_{\sigma(k)} = I_{n_x} - \Lambda_{\sigma(k)}C_{\sigma(k)}$, Eqs. (44a) and (44b) are obtained and the proof is complete. $\square$

5.2. Optimal switched correction matrix design

Following the same methodology as in the previous section, the size of the intersection zonotope $\hat{\mathbb{X}}_{k+1}$ is measured by the W_i-Radius as follows

$$
\begin{aligned}
l_k^W &= \max_{z \in \mathbf{B}^{(q+n_x+2n_y)}} \left\| \hat{H}_k(\Lambda_{\sigma(k)})z \right\|_{2,W_{\sigma(k)}}^2 \\
&= \max_{z \in \mathbf{B}^{(q+n_x+2n_y)}} z^T \hat{H}_k^T(\Lambda_{\sigma(k)})W_{\sigma(k)}\hat{H}_k(\Lambda_{\sigma(k)})z
\end{aligned} \tag{52}
$$

where $W_{\sigma(k)} = W_i$, $\forall i \in \{1, \ldots, N\}$ is the weighting matrix for the ith subsystem. If there exists a scalars $\alpha_{\sigma(k)}$ and $\gamma_{\sigma(k)}$ associated with each subsystem $\sigma(k) = i$ such that

$$
\Delta_{k-1}^{l_W} \leq -\alpha_{\sigma(k)} l_{k-1}^W + \gamma_{\sigma(k)}\epsilon_{\sigma(k)} \tag{53}
$$

where $\epsilon_{\sigma(k)}$ is a positive switched constant that represents the maximum influence of disturbances and measurement noises:

$$
\epsilon_{\sigma(k)} = \max_{s_1 \in \mathbf{B}^{n_\omega}} \left\| D_{\sigma(k)}s_1 \right\|_2^2 + \max_{s_2 \in \mathbf{B}^{n_v}} \left\| F_{\sigma(k)}s_2 \right\|_2^2 \tag{54}
$$

then, the size of the zonotope $\hat{\mathbb{X}}_k$ is decreasing. If Eq. (53) holds, then for time instant $k \to \infty$, we have

$$
l_\infty^W = \frac{\gamma_i \epsilon_i}{\alpha_i}, \ \forall i \in \{1, \ldots, N\} \tag{55}
$$

To minimize the W_i-Radius (i.e l_∞^W), the smallest performance level gain γ_i is sought for the ith subsystem. It is clear from Eq. (55) that the gain γ_i, $\forall i \in I$ provides a tighter information in terms of the effect of ε_i, $\forall i \in I$ on the W_i-Radius l_∞^W. This leads to solve the following optimization problem:

Theorem 6. *Given the intersection zonotope $\hat{\mathbb{X}}_k = \langle \hat{p}_k, \hat{H}_k \rangle$ in (Eq. 44). Inequality Eq. (53) holds if there exists a matrix $Y_i \in \mathbb{R}^{n_x \times n_y}$, a positive definite matrix $W_i \in \mathbb{R}^{n_x \times n_x}$, for given scalars $\alpha_i \in (0, 1)$, $\gamma >$ and $\epsilon_i > 0$ such that the following LMI problem holds*

$$
\min_{\gamma_i, W_i, Y_i} \gamma
$$

$$
\gamma_i \leq \gamma, \quad \forall i \in \{1, \ldots, N\} \tag{56}
$$

$$\begin{bmatrix} (\alpha_i - 1)W_i & * & * & * & * \\ 0 & -\gamma_i D_i^T D_i & * & * & * \\ 0 & 0 & -\gamma_i F_i^T F_i & * & * \\ 0 & 0 & 0 & 0 & * \\ (W_i - Y_i C_i)P_i A_i & (W_i - Y_i C_i)P_i D_i & (W_i - Y_i C_i)M_i F_i & Y_i F_i & -W_i \end{bmatrix} \preceq 0, \forall i \in I \tag{57}$$

with $Y_i = W_i \Lambda_i$.

Proof. Let $\Delta_{k-1}^{l_W} = l_k^W - l_{k-1}^W$, and, $z = \begin{bmatrix} \bar{z}^T & s_1^T & s_2^T & s_3^T \end{bmatrix}^T \in \mathbf{B}^{q+n_x+2n_y}$ with $\bar{z} \in \mathbf{B}^q$, $s_1 \in \mathbf{B}^{n_x}$, $s_2 \in \mathbf{B}^{n_y}$ and $s_3 \in \mathbf{B}^{n_y}$, then using Eq. (52) we have

$$\Delta_{k-1}^{l_W} = \max_{z \in \mathbf{B}^{(q+n_x+2n_y)}} \left\| \hat{H}_k(\Lambda_{\sigma(k)})z \right\|_{2,W_{\sigma(k)}}^2 - \max_{\hat{z} \in \mathbf{B}^q} \left\| \overline{H}_{k-1}\bar{z} \right\|_{2,W_{\sigma(k)}}^2 \tag{58}$$

this leads to

$$\begin{aligned} \Delta_{k-1}^{l_W} &= \max_{\bar{z} \in \mathbf{B}^q, s_1 \in \mathbf{B}^{n_x}, s_2 \in \mathbf{B}^{n_y}, s_3 \in \mathbf{B}^{n_y}} \left(\left\| \hat{H}_k(\Lambda_{\sigma(k)})z \right\|_{2,W_{\sigma(k)}}^2 - \left\| \overline{H}_k(\Lambda_{\sigma(k)})\bar{z} \right\|_{2,W_{\sigma(k)}}^2 \right) \\ &= \max_{\bar{z} \in \mathbf{B}^q, s_1 \in \mathbf{B}^{n_x}, s_2 \in \mathbf{B}^{n_y}, s_3 \in \mathbf{B}^{n_y}} \left(\begin{bmatrix} \bar{z} \\ s_1 \\ s_2 \\ s_3 \end{bmatrix}^T \hat{H}_k^T(\Lambda_{\sigma(k)}) W_{\sigma(k)} \hat{H}_k(\Lambda_{\sigma(k)}) \begin{bmatrix} \bar{z} \\ s_1 \\ s_2 \\ s_3 \end{bmatrix} - \right. \\ &\quad \left. \bar{z}^T \overline{H}_{k-1}^T W_{\sigma(k)} \overline{H}_{k-1} \bar{z} \right) \end{aligned} \tag{59}$$

By adding and subtracting the terms $\max_{\bar{z} \in \mathbf{B}^q} \alpha_{\sigma(k)} \left\| \overline{H}_{k-1}\bar{z} \right\|_{2,W_{\sigma(k)}}^2$ and $-\gamma_{\sigma(k)}\epsilon_{\sigma(k)}$ where $\epsilon_{\sigma(k)}$ is given by Eqs. (54), (59) is rewritten as

$$\begin{aligned} \Delta_{k-1}^{l_W} &= \max_{\bar{z} \in \mathbf{B}^q, s_1 \in \mathbf{B}^{n_x}, s_2 \in \mathbf{B}^{n_y}, s_3 \in \mathbf{B}^{n_y}} \left(\begin{bmatrix} \bar{z} \\ s_1 \\ s_2 \\ s_3 \end{bmatrix}^T \hat{H}_k^T(\Lambda_{\sigma(k)}) W_{\sigma(k)} \hat{H}_k(\Lambda_{\sigma(k)}) \begin{bmatrix} \bar{z} \\ s_1 \\ s_2 \\ s_3 \end{bmatrix} + \right. \\ &\alpha_{\sigma(k)} \bar{z}^T \overline{H}_{k-1}^T W_{\sigma(k)} \overline{H}_{k-1} \bar{z} - \bar{z}^T \overline{H}_{k-1}^T W_{\sigma(k)} \overline{H}_{k-1} \bar{z} - \gamma_{\sigma(k)} s_1^T D_{\sigma(k)}^T D_{\sigma(k)} s_1 - \\ &\left. \gamma_{\sigma(k)} s_2^T F_{\sigma(k)}^T F_{\sigma(k)} s_2 \right) - \max_{\bar{z} \in \mathbf{B}^q} \alpha_{\sigma(k)} \left\| \overline{H}_{k-1}\bar{z} \right\|_{2,W_{\sigma(k)}}^2 + \gamma_{\sigma(k)}\epsilon_{\sigma(k)} \end{aligned} \tag{60}$$

Substituting Eq. (44b) into Eq. (60), we get

$$\begin{aligned} &\max_{\bar{z} \in \mathbf{B}^q, s_1 \in \mathbf{B}^{n_x}, s_2 \in \mathbf{B}^{n_y}, s_3 \in \mathbf{B}^{n_y}} \left(\begin{bmatrix} \overline{H}_{k-1}\bar{z} \\ s_1 \\ s_2 \\ s_3 \end{bmatrix}^T \left(\Theta_{\sigma(k)}^T W_{\sigma(k)} \Theta_{\sigma(k)} + \right. \right. \\ &\left. \left. \begin{bmatrix} (\alpha_{\sigma(k)} - 1)W_{\sigma(k)} & 0 & 0 & 0 \\ 0 & -\gamma_{\sigma(k)} D_{\sigma(k)}^T D_{\sigma(k)} & 0 & 0 \\ 0 & 0 & -\gamma_{\sigma(k)} F_{\sigma(k)}^T F_{\sigma(k)} & 0 \\ 0 & 0 & 0 & 0 \end{bmatrix} \right) \begin{bmatrix} \overline{H}_{k-1}\bar{z} \\ s_1 \\ s_2 \\ s_3 \end{bmatrix} \right) \\ &- \max_{\bar{z} \in \mathbf{B}^q} \alpha_{\sigma(k)} \left\| \overline{H}_{k-1}\bar{z} \right\|_{2,W_{\sigma(k)}}^2 + \gamma_{\sigma(k)}\epsilon_{\sigma(k)} \end{aligned} \tag{61}$$

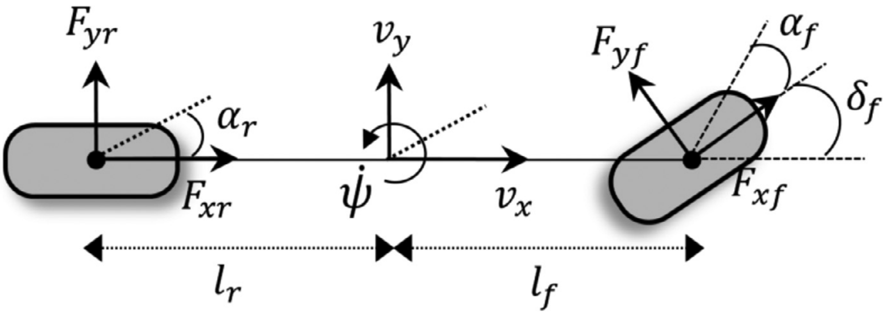

Fig. 4. Schematic diagram of the vehicle bicycle model.

where $\Theta_{\sigma(k)} = \begin{bmatrix} T_{\sigma(k)}P_{\sigma(k)}A_{\sigma(k)} \\ T_{\sigma(k)}P_{\sigma(k)}D_{\sigma(k)} \\ T_{\sigma(k)}M_{\sigma(k)}F_{\sigma(k)} \\ \Lambda_{\sigma(k)}F_{\sigma(k)} \end{bmatrix}$. If the following inequality holds $\forall i \in I$

$$\begin{bmatrix} (\alpha_{\sigma(k)} - 1)W_{\sigma(k)} & 0 & 0 & 0 \\ 0 & -\gamma_{\sigma(k)}D^T_{\sigma(k)}D_{\sigma(k)} & 0 & 0 \\ 0 & 0 & -\gamma_{\sigma(k)}F^T_{\sigma(k)}F_{\sigma(k)} & 0 \\ 0 & 0 & 0 & 0 \end{bmatrix} + \Theta^T_{\sigma(k)}W_{\sigma(k)}\Theta_{\sigma(k)} \prec 0 \tag{62}$$

which is equivalent by Schur complement to Eq. (57), then

$$\Delta^{l_W}_{k-1} \leq -\alpha_{\sigma(k)} l^W_{k-1} + \gamma_{\sigma(k)}\epsilon_{\sigma(k)} \tag{63}$$

from which we prove that satisfying Eq. (57) is enough to fulfill the condition Eq. (53). Furthermore, the tight size of the intersection zonotope must be sought, hence the introduction of the conditions Eq. (56) which completes the proof of Theorem 6. □

6. Application to vehicle sideslip angle estimation

Vehicle lateral dynamics may be modeled using a two degree of freedom (2-DOF) model known as the "bicycle model" to describe the lateral and yaw motions [55]. The vehicle's left and right wheels are grouped together to form a single steerable front wheel and rear wheel with negligible inertia as shown in Fig. 4. This representation, also known as "single track model", has been proven to perfectly represent the vehicle lateral dynamics behavior and especially when evaluating sideslip angle and studying lateral efforts. In this model, roll movement is neglected and vertical motions are ignored.

The two-dimensional model describing the vehicle lateral behavior can be represented by the following differential equations:

$$\begin{cases} mv_x\dot{\beta} + mv_x\dot{\psi} = F_{yf} + F_{yr} \\ I_z\ddot{\psi} = l_fF_{yf} - l_rF_{yr} \end{cases} \tag{64}$$

where m, I_z, are the mass and the yaw moment, v_x is the longitudinal velocity, β and $\dot{\psi}$ are vehicle sideslip angle and yaw rate, l_f, l_r are distances from front and rear axle to the center of gravity (CG), while F_{yf} and F_{yr} are lateral tire force of front and rear tires. The lateral forces F_{yf} and F_{yr} are assumed to be proportional to the tire slip angles α_f and α_r for small sideslip angle [56]:

$$\begin{cases} F_{yf} = c_f \alpha_f = c_f(\delta_f - \beta - \frac{lf}{v_x}\dot{\psi}) \\ F_{yr} = c_r \alpha_r = c_r(-\beta + \frac{lr}{v_x}\dot{\psi}) \end{cases} \tag{65}$$

where c_f, c_r are the cornering stiffness of front and rear tires while δ_f represents the front steering angle.

Gathering Eqs. (64) and (65) and choosing β and $\dot{\psi}$, as state variables, leads to the following state equations:

$$\begin{bmatrix} \dot{\beta} \\ \ddot{\psi} \end{bmatrix} = \begin{bmatrix} -\frac{c_f + c_r}{m v_x} & \frac{c_r l_r - c_f l_f}{m v_x^2} - 1 \\ \frac{c_r l_r - c_f l_f}{I_z} & -\frac{c_r l_r^2 + c_f l_f^2}{I_z v_x} \end{bmatrix} \begin{bmatrix} \beta \\ \dot{\psi} \end{bmatrix} + \begin{bmatrix} \frac{c_f}{m v_x} \\ \frac{c_f l_f}{Iz} \end{bmatrix} \delta_f \tag{66}$$

The bicycle model Eq. (66) was first discretized using zero order hold method. Next, a switched representation of the vehicle model Eq. (66) is considered to take into account vehicle longitudinal velocity variations. A switched system where each subsystem operates around a given constant longitudinal velocity value (for example, three subsystems defined for low, average and high longitudinal speed) is adopted in this paper. Then, a switching signal depending on the measured longitudinal velocity is considered. Note that, all vehicle model parameters are assumed to be known. Environmental disturbances as well as non-modelled effects (unknown wind gust, cornering stiffness variations) are added to the vehicle model through additive state disturbance and measurement noise vectors $\omega_{\sigma(k)}$ and $\varepsilon_{\sigma(k)}$. The available measurements are yaw rate $\dot{\psi}$, longitudinal velocity v_x and front steering angle δ_f. The real data used in the validation process are based on measurements obtained from tests carried out on an instrumented vehicle of the LIVIC[1] laboratory in a test track located in the city of Versailles-Satory, France (Fig. 5). The track is 3.5km length with various curvatures ranging between $30m$ and $600m$.

The vehicle is equipped with several exteroceptive and proprioceptive sensors. Here, we present, in a succinct manner, the sensors used to collect the measurements of the variables required in this study:

- Yaw rate $\dot{\psi}$ and lateral acceleration a_y are measured by a three-axis inertial unit which provides the accelerations and rotational velocities along the three axes (roll, pitch and yaw).
- Steering angle input δ_f is provided by an absolute optical encoder.
- Longitudinal velocity v_x is measured by an odometer.
- Sideslip angle β is obtained using a Correvit sensor. The measure is not used in the observer design. It serves only for validation.

6.1. Case 1

In order to examine the performance of the proposed design, a first experimental data set is used, where three subsystems are defined for $v_x^1 = 8.50$ m/s, $v_x^2 = 13.55$ m/s and $v_x^3 = 18.05$

[1] Laboratory for Vehicle Infrastructure Driver Interactions.

Fig. 5. Test track (Satory, France) [57].

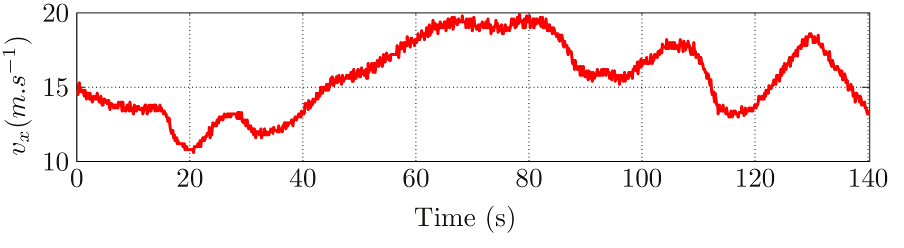

Fig. 7. Longitudinal velocity v_x.

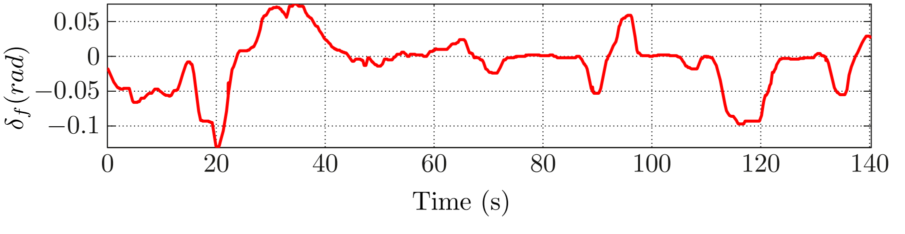

Fig. 6. Steering angle δ_f.

m/s. The choice between the modes is done according to vehicle longitudinal measure in Fig. 7. The switching rule is then designed as follows:

$$\sigma(t) = \begin{cases} 1 & if \;\; 6\,\text{m/s} < v_x \leq 11\,\text{m/s} \\ 2 & if \;\; 11\,\text{m/s} < v_x \leq 16\,\text{m/s} \\ 3 & if \;\; 16\,\text{m/s} < v_x \leq 20\,\text{m/s} \end{cases} \tag{67}$$

where the three modes correspond to three different driving conditions: low, medium, and high longitudinal speed. Steering angle and the considered switching law are shown in Figs. 6 and 8. The disturbance and noise vectors satisfy $|\omega_k| \leq \begin{bmatrix} 0.002 & 0.01 \end{bmatrix}^T$ and $|v_k| \leq 0.03$. The

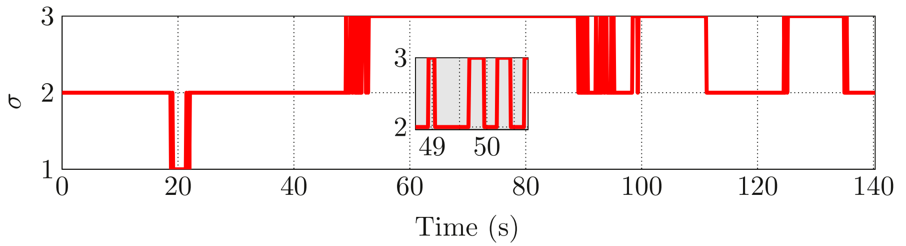

Fig. 8. Switching signal $\sigma(k)$.

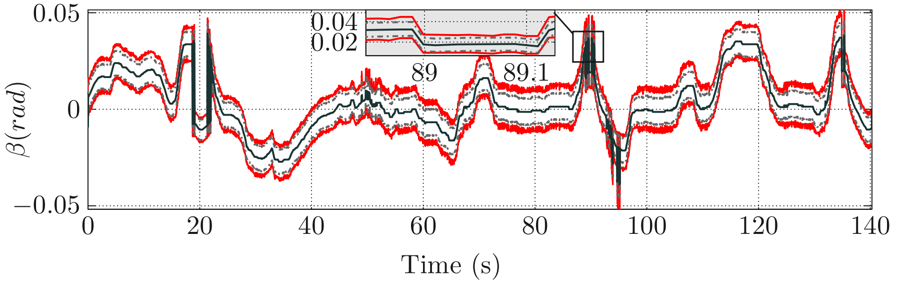

Fig. 9. Interval estimation of vehicle side slip angle β using Theorem 2 (dashed gray line) and optimization problem (29) (red line). (For interpretation of the references to colour in this figure legend, the reader is referred to the web version of this article.)

switched correction matrices $\Lambda_{\sigma(k)}$ and $\tilde{\Lambda}_{\sigma(k)}$ are obtained by solving constraints Eqs. (20) and (29), respectively. The scalar β in Eq. (29) and $(1-\alpha_{\sigma(k)})$ in Eq. (20) are set equal for comparison purpose. This allows to show the usefulness of adding the gain $\gamma_{\sigma(k)}$ in the new formulation (20). Therefore, the following feasible solutions are obtained by solving LMI constraints Eq. (29) and Eq. (20) for $\tilde{\alpha}_1 = \tilde{\alpha}_2 = \tilde{\alpha}_3 = 0.1$ and $\alpha_1 = \alpha_2 = \alpha_3 = 0.9$:

$$\Lambda_1 = \begin{bmatrix} -0.0003 \\ 0.0996 \end{bmatrix}, \quad \Lambda_2 = \begin{bmatrix} -0.0071 \\ 0.1460 \end{bmatrix}, \quad \Lambda_3 = \begin{bmatrix} -0.0002 \\ 0.1339 \end{bmatrix}$$
$$\tilde{\Lambda}_1 = \begin{bmatrix} 0.0113 \\ 0.5817 \end{bmatrix}, \quad \tilde{\Lambda}_2 = \begin{bmatrix} 0.0233 \\ 0.7969 \end{bmatrix}, \quad \tilde{\Lambda}_3 = \begin{bmatrix} 0.0240 \\ 0.8903 \end{bmatrix}$$

The results of interval estimation are depicted in Figs. 9 and 10. As shown, the proposed method allows to obtain an accurate and tight interval estimation of vehicle state variables than the method in [44]. The attenuation of disturbance and measurement noise effects can clearly be observed. Figure 11 and 12 compare interval width for sideslip angle $e_\beta = \overline{\beta} - \underline{\beta}$ and yaw rate $e_{\dot{\psi}} = \overline{\dot{\psi}} - \underline{\dot{\psi}}$. It can be noticed that the proposed estimation framework can handle additive uncertainties more effectively than the conventional methods.

The state estimation using the zonotopic observer and the set-membership approach is compared in order to validate the obtained mathematical equivalence. Using Theorem 2, the switched observer gains L_i, $\forall i \in I$ are obtained for $\tilde{\alpha}_1 = \tilde{\alpha}_2 = \tilde{\alpha}_3 = 0.1$ and $\alpha_1 = \alpha_2 = \alpha_3 = 0.9$:

$$L_1 = \begin{bmatrix} -0.0003 \\ 0.0996 \end{bmatrix}, \quad L_2 = \begin{bmatrix} -0.0071 \\ 0.1460 \end{bmatrix}, \quad L_3 = \begin{bmatrix} -0.0002 \\ 0.1339 \end{bmatrix}$$

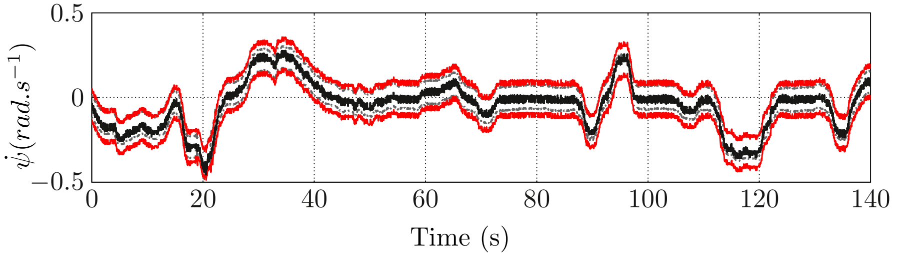

Fig. 10. Interval estimation of vehicle yaw rate $\dot{\psi}$ using Theorem 2 (dashed gray line) and optimization problem Eq. (29) (red line). (For interpretation of the references to colour in this figure legend, the reader is referred to the web version of this article.)

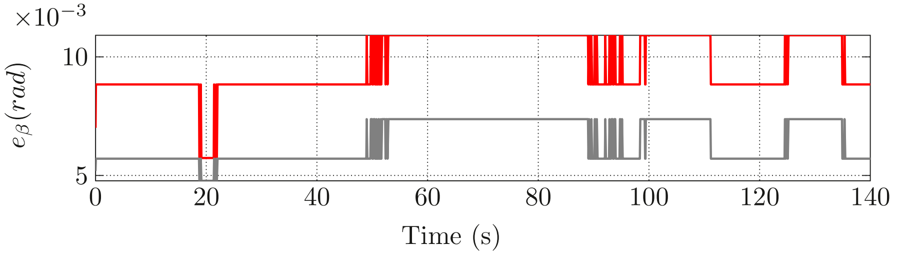

Fig. 11. Interval error e_β using Theorem 2 (gray line) and optimization problem Eq. (29) (red line). (For interpretation of the references to colour in this figure legend, the reader is referred to the web version of this article.)

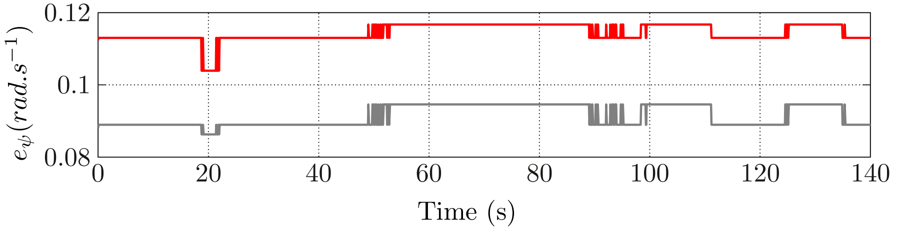

Fig. 12. Interval error $e_{\dot{\psi}}$ using Theorem 2 (gray line) and optimization problem Eq. (29) (red line). (For interpretation of the references to colour in this figure legend, the reader is referred to the web version of this article.)

As the computation time needed for solving optimization problems is the most important matter in assessing the efficiency of an algorithm. A comparison in terms of the computational time required for solving the optimization problem Eq. (29) and the one presented in Theorem 2 was done. Experiment were conducted using an Intel Core i7 with a processor running at 2.9 GHz in MATLAB R2016a running under Windows 10. The results are presented in Fig. 13.

In terms of the required computation time, the optimization problem in Eq. (29) requires a highest computational demand compared to Theorem 2 (Three time larger for a 2nd order system). The proposed design strategy exhibits very small computation time. Thus, the proposed method outperforms the conventional design significantly.

The interval estimation of the vehicle sideslip angle and yaw rate are compared to those obtained using SMA and illustrated in Figs. 14 and 15. Both approaches are able to provide interval state estimation results with the same performance as have been shown in Section 4.

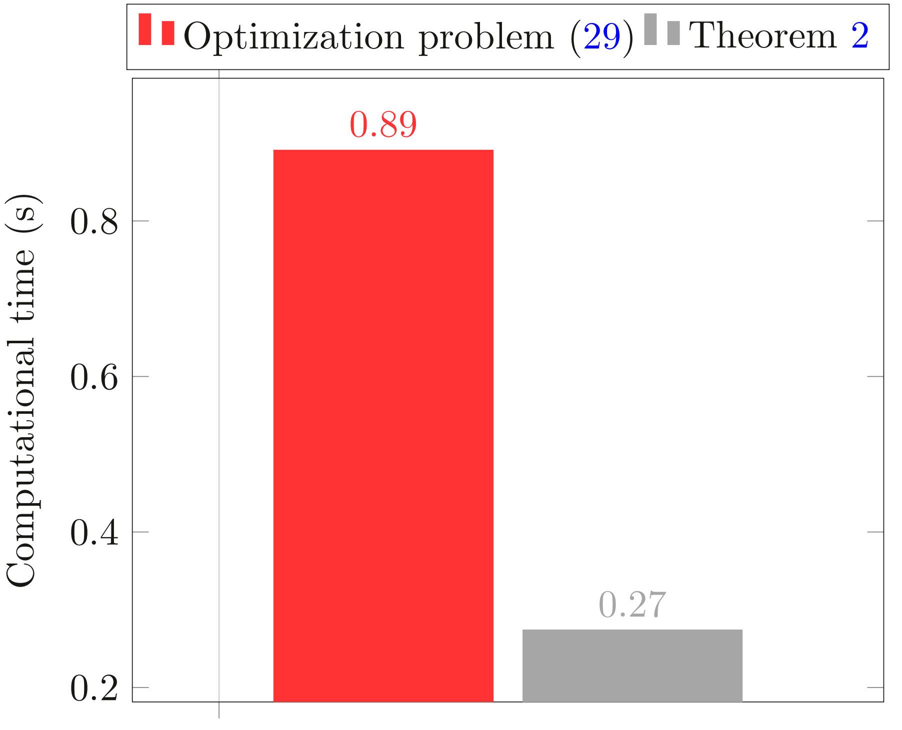

Fig. 13. Computation time required by each method.

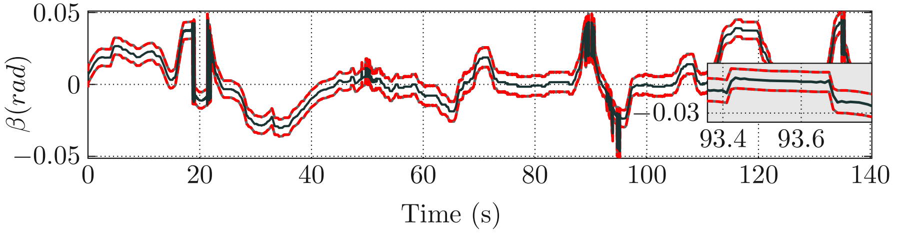

Fig. 14. Interval estimation of vehicle side slip angle β using Zonotopic Observer (dashed gray line) and Set-Membership Approach (red line). (For interpretation of the references to colour in this figure legend, the reader is referred to the web version of this article.)

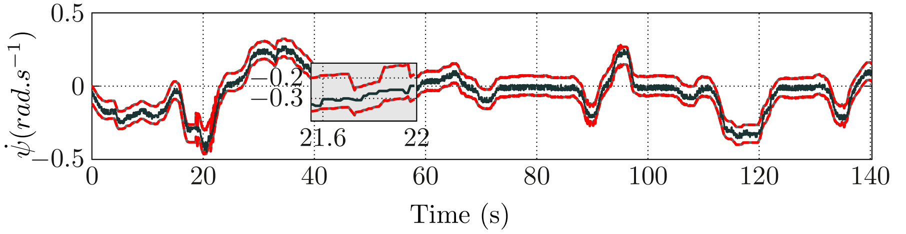

Fig. 15. Interval estimation of vehicle yaw rate $\dot{\psi}$ using Zonotopic Observer (dashed gray line) and Set-Membership Approach (red line). (For interpretation of the references to colour in this figure legend, the reader is referred to the web version of this article.)

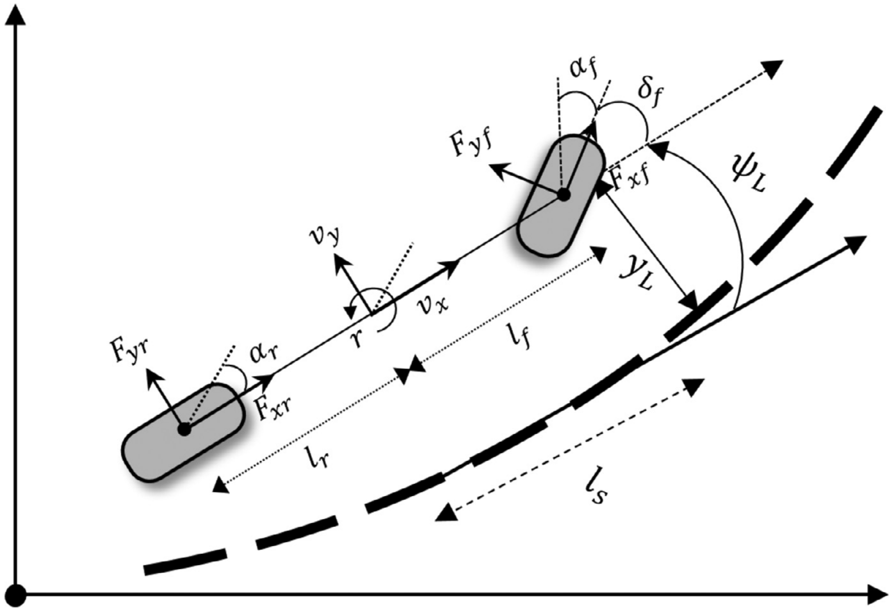

Fig. 16. Vision system measurement.

6.2. Case 2

In order to illustrate the inclusion of the unknown input improvement presented in Section 5, vehicle lateral dynamics in a cornering lane is considered. The vision system model providing vehicle angular and lateral displacements from the center-line at a look ahead distance l_s (See Fig. 16) is used. These measurements are extracted from images obtained with a suitable vision system, taking into consideration the motion of the vehicle and changes in the road geometry.

The equations describing the evolution of the vision system measurement are given as follows:

$$\begin{cases} \dot{\psi}_L = \dot{\psi} - v_x\rho \\ \dot{y}_L = v_y + v_x\psi_L + l_s(\dot{\psi} - v_x\rho) \end{cases} \tag{68}$$

which can be rewritten in the following state representation form:

$$\begin{bmatrix} \dot{\psi}_L \\ \dot{y}_L \end{bmatrix} = \begin{bmatrix} 0 & 0 \\ 0 & v_x \end{bmatrix} \begin{bmatrix} \psi_L \\ y_L \end{bmatrix} + \begin{bmatrix} 0 & 1 \\ 1 & l_s \end{bmatrix} \begin{bmatrix} v_y \\ r \end{bmatrix} + \begin{bmatrix} -v_x \\ -l_s v_x \end{bmatrix} \rho \tag{69}$$

where y_L and ψ_L are the offset and angular displacements at a look ahead distance l_s, while, ρ represents the road curvature.

Combining the two degrees of freedom model describing the vehicle yaw and lateral motions Eq. (64) together with the equations describing the evolution of the vehicle angular and lateral displacements Eq. (69), leads to a single dynamical system subject to the road curvature as an unknown input. By adopting a switched representation of the resulted discretized vehicle model and considering that the state and measurement equations are subject to additive

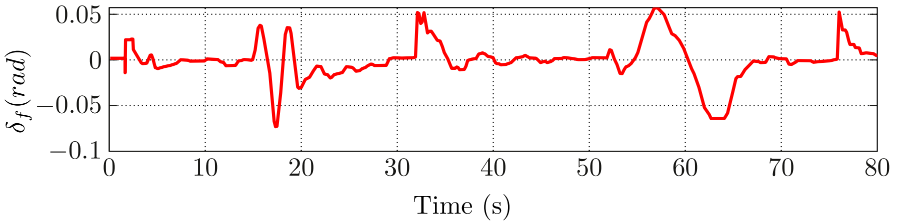

Fig. 17. Steering angle.

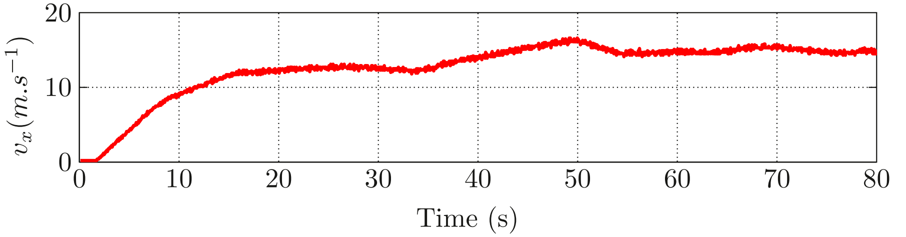

Fig. 18. Longitudinal velocity.

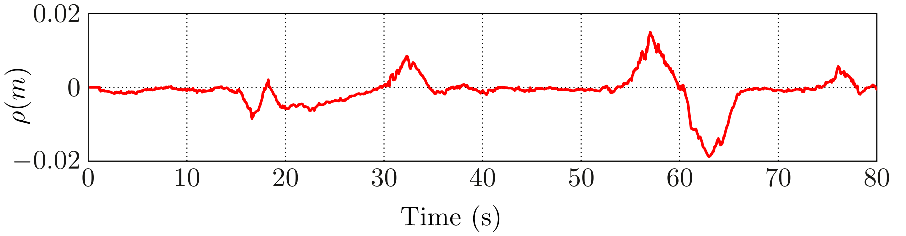

Fig. 19. Road curvature.

disturbance and noise, an uncertain discrete-time switched system of the form Eq. (37) is obtained.

A second set of experimental data is used to evaluate the proposed unknown input set-membership state estimator. The measurements are acquired using the same prototype vehicle described above. The lateral offset and angular displacements y_L and ψ_L are measured using clustering of a video, camera mounted under the mirror of the vehicle, and vision algorithms. For the simulation scenario, three subsystems are defined for $v_x^1 = 3.1m/s$, $v_x^2 = 8.5m/s$ and $v_x^3 = 13.75m/s$. The steering angle, longitudinal velocity, road curvature and the considered switching law are shown in Figs. 17–20.

The disturbance and noise vectors satisfy $|\omega_k| \leq \begin{bmatrix} 0.002 & 0.004 & 0.02 & 0.003 \end{bmatrix}^T$ and $|v_k| \leq \begin{bmatrix} 0.005 & 0.04 & 0.003 \end{bmatrix}^T$. The switched matrices $M_{\sigma(k)}$ and $P_{\sigma(k)}$ are obtained by solving constraints Eq. (39) using the generalized inverse. Therefore, the following feasible solutions are considered:

$$P_1 = \begin{bmatrix} 1 & -0.0100 & -0.0013 & 0.0010 \\ 0 & 1.0100 & 0.0013 & -0.0010 \\ 0 & -0.0100 & 0.6178 & -0.4846 \\ 0 & -0.0100 & -0.4869 & 0.3819 \end{bmatrix}, \; M_1 = \begin{bmatrix} 0.0100 & 0.0013 & -0.0010 \\ -0.0100 & -0.0013 & 0.0010 \\ 0.0100 & 0.3822 & 0.4846 \\ 0.0100 & 0.4869 & 0.6181 \end{bmatrix}$$

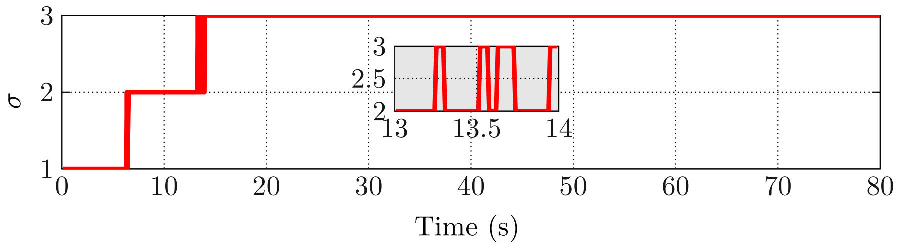

Fig. 20. Switching signal.

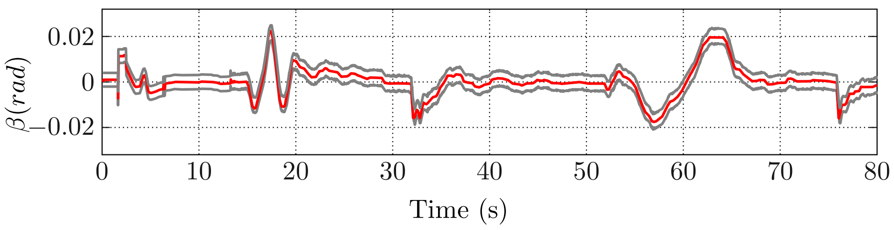

Fig. 21. Interval estimation of sideslip angle.

$$P_2 = \begin{bmatrix} 1 & -0.0200 & -0.0108 & 0.0041 \\ 0 & 0.9800 & 0.0241 & -0.0092 \\ 0 & -0.0200 & 0.8782 & -0.3345 \\ 0 & 0 & -0.3435 & 0.1309 \end{bmatrix}, \quad M_2 = \begin{bmatrix} 0.0200 & 0.0108 & -0.0041 \\ 0.0200 & -0.0241 & 0.0092 \\ 0.0200 & 0.1218 & 0.3345 \\ 0 & 0.3435 & 0.8691 \end{bmatrix}$$

$$P_3 = \begin{bmatrix} 1 & -0.0200 & -0.0140 & 0.0036 \\ 0 & 1.0200 & 0.0140 & -0.0036 \\ 0 & -0.0200 & 0.9254 & -0.2350 \\ 0 & -0.0200 & -0.2150 & 0.0546 \end{bmatrix}, \quad M_3 = \begin{bmatrix} 0.0200 & 0.0140 & -0.0036 \\ -0.0200 & -0.0140 & 0.0036 \\ 0.0200 & 0.0746 & 0.2350 \\ 0.0200 & 0.2150 & 0.9454 \end{bmatrix}$$

The optimal correction switched matrix $\Lambda_{\sigma(k)}$ is designed by solving the optimization problem in Theorem 6 for a reduction operator $q = 40$. The optimal solution is given by

$$\Lambda_1 = \begin{bmatrix} -0.0116 & -0.0052 & -0.0040 \\ 0.4104 & 0.0007 & -0.0006 \\ -0.3159 & 0.1211 & -0.6489 \\ -0.0075 & -0.0004 & 0.9969 \end{bmatrix}, \quad \Lambda_2 = \begin{bmatrix} -0.0500 & -0.0116 & -0.0018 \\ 0.6279 & -0.0001 & -0.0262 \\ 0.1061 & 0.4455 & -1.3249 \\ 0.0159 & -0.0030 & 0.9928 \end{bmatrix}$$

$$\Lambda_3 = \begin{bmatrix} -0.0154 & -0.0142 & 0.0024 \\ 0.9368 & 0.0236 & 0.0967 \\ -0.0289 & 0.9374 & -0.2064 \\ -0.0013 & 0.0005 & 1.0018 \end{bmatrix}$$

for $\alpha_1 = \alpha_2 = \alpha_3 = 0.99$. The results of interval estimation are depicted in Figs. 21–24 which shows that the proposed method allows to obtain a very accurate interval estimation of vehicle state variables.

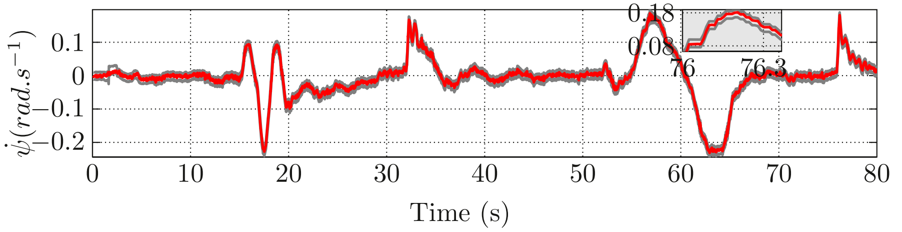

Fig. 22. Interval estimation of yaw rate.

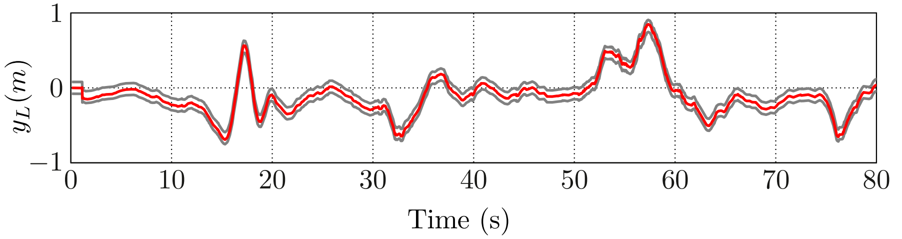

Fig. 23. Interval estimation of offset displacement.

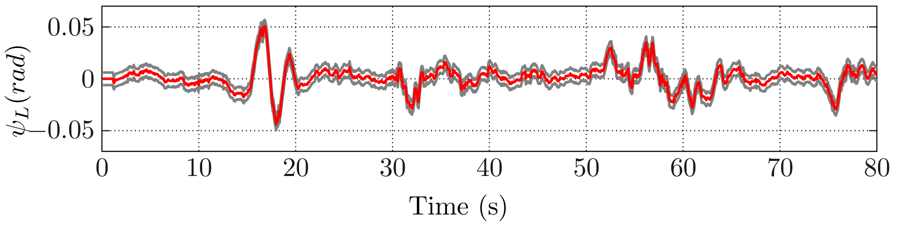

Fig. 24. Interval estimation of angular displacement.

7. Conclusion

This paper has presented a new zonotopic set-membership estimation approach for uncertain switched systems. As it has been demonstrated by application example, Theorem 2 provides much simpler and less conservative conditions than the traditional guaranteed state estimation based on W_i-radius minimization. The synthesized solution has less complexity and requires shorter computational time. It has been shown that the proposed set-membership is equivalent to a zonotopic observer. An extension to set-membership state estimation of switched systems subject to both unknown and bounded inputs is presented. This extension allows to deal with several limitations. Namely, the relaxation of the strong unknown input decoupling assumption (defined as rank constraint, i.e. $rank(CE_i) = rank(E_i)$, $\forall i \in I$). In addition, the proposed method can also be considered to deal with unknown and unbounded disturbances which present one of the weakness in the set-based approaches. The suggested methods are efficiently applied to estimate the vehicle sideslip angle. Performance of the proposed algorithms are illustrated through simulations and comparisons with experimental data.

Declaration of Competing Interest

The authors declare that they have no known competing financial interests or personal relationships that could have appeared to influence the work reported in this paper.

References

[1] P.J. Antsaklis, A brief introduction to the theory and applications of hybrid systems, in: Proc IEEE, Special Issue on Hybrid Systems: Theory and Applications, Citeseer, 2000.

[2] D. Liberzon, Switching in Systems and Control, Springer Science & Business Media, 2012.

[3] D. Liberzon, A.S. Morse, Basic problems in stability and design of switched systems, IEEE Control Syst. 19 (5) (1999) 59–70.

[4] R. Goebel, R.G. Sanfelice, A.R. Teel, Hybrid dynamical systems, IEEE Control Syst. 29 (2) (2009) 28–93.

[5] P. Mhaskar, N.H. El-Farra, P.D. Christofides, Predictive control of switched nonlinear systems with scheduled mode transitions, IEEE Trans. Automat. Control 50 (11) (2005) 1670–1680.

[6] J. Liu, S. Laghrouche, M. Harmouche, M. Wack, Adaptive-gain second-order sliding mode observer design for switching power converters, Control Eng. Pract. 30 (2014) 124–131.

[7] H. Lin, P.J. Antsaklis, Stability and persistent disturbance attenuation properties for a class of networked control systems: switched system approach, Int. J. Control 78 (18) (2005) 1447–1458.

[8] A. Zin, O. Sename, L. Dugard, Switched H_∞ control strategy of automotive active suspensions, IFAC Proc. Vol. 38 (1) (2005) 198–203.

[9] H. Yang, B. Jiang, V. Cocquempot, H. Zhang, Stabilization of switched nonlinear systems with all unstable modes: application to multi-agent systems, IEEE Trans. Automat. Control 56 (9) (2011) 2230–2235.

[10] A.A. Agrachev, D. Liberzon, Lie-algebraic conditions for exponential stability of switched systems, in: Decision and Control, 1999. Proceedings of the 38th IEEE Conference on, vol. 3, IEEE, 1999, pp. 2679–2684.

[11] L. Vu, D. Chatterjee, D. Liberzon, Input-to-state stability of switched systems and switching adaptive control, Automatica 43 (4) (2007) 639–646.

[12] H. Lin, P.J. Antsaklis, Stability and stabilizability of switched linear systems: a survey of recent results, IEEE Trans. Automat. Control 54 (2) (2009) 308–322.

[13] Z. Sun, S.S. Ge, T.H. Lee, Controllability and reachability criteria for switched linear systems, Automatica 38 (5) (2002) 775–786.

[14] G. Xie, L. Wang, Necessary and sufficient conditions for controllability and observability of switched impulsive control systems, IEEE Trans. Automat. Control 49 (6) (2004) 960–966.

[15] A. Bemporad, G. Ferrari-Trecate, M. Morari, Observability and controllability of piecewise affine and hybrid systems, IEEE Trans. Automat. Control 45 (10) (2000) 1864–1876.

[16] Z.G. Li, C.Y. Wen, Y.C. Soh, Observer-based stabilization of switching linear systems, Automatica 39 (3) (2003) 517–524.

[17] A. Alessandri, P. Coletta, Design of Luenberger observers for a class of hybrid linear systems, in: International Workshop on Hybrid Systems: Computation and Control, Springer, 2001, pp. 7–18.

[18] G. Ackerson, K. Fu, On state estimation in switching environments, IEEE Trans. Automat. Control 15 (1) (1970) 10–17.

[19] A. Balluchi, L. Benvenuti, M.D. Di Benedetto, A.L. Sangiovanni-Vincentelli, Design of observers for hybrid systems, in: International Workshop on Hybrid Systems: Computation and Control, Springer, 2002, pp. 76–89.

[20] H. Saadaoui, N. Manamanni, M. Djemai, J.-P. Barbot, T. Floquet, Exact differentiation and sliding mode observers for switched lagrangian systems, Nonlinear Anal. Theory MethodsAppl. 65 (5) (2006) 1050–1069.

[21] F.J. Bejarano, A. Pisano, Switched observers for switched linear systems with unknown inputs, IEEE Trans. Automat. Control 56 (3) (2011) 681–686.

[22] J. Van Gorp, M. Defoort, K.C. Veluvolu, M. Djemai, Hybrid sliding mode observer for switched linear systems with unknown inputs, J. Franklin Inst. 351 (7) (2014) 3987–4008.

[23] J. Yang, Y. Chen, Z. Zheng, W. Qian, Robust adaptive state estimation for uncertain nonlinear switched systems with unknown inputs, Trans. Inst. Meas. Control 40 (4) (2018) 1082–1091.

[24] H. Saadaoui, J. De Leon, M. Djemai, N. Manamanni, J. Barbot, High order sliding mode and adaptive observers for a class of switched systems with unknown parameter: a comparative study, in: Proceedings of the 45th IEEE Conference on Decision and Control, IEEE, 2006, pp. 5555–5560.

[25] L. Islem, T. Asma, Z. Nadia, Hybrid sliding mode observer for uncertain linear switching system with actuator faults, Trans. Inst. Meas. Control (2019). 0142331219856198
[26] L. Zhang, P. Shi, C. Wang, H. Gao, Robust H_∞ filtering for switched linear discrete-time systems with polytopic uncertainties, Int. J. Adapt. Control Signal Process. 20 (6) (2006) 291–304.
[27] J. Qiu, G. Feng, J. Yang, Robust mixed H_2/H_∞ filtering design for discrete-time switched polytopic linear systems, IET Control Theory Appl. 2 (5) (2008) 420–430.
[28] D. Du, B. Jiang, P. Shi, S. Zhou, $\mathcal{H}_\infty$ filtering of discrete-time switched systems with state delays via switched Lyapunov function approach, IEEE Trans. Automat. Control 52 (8) (2007) 1520–1525.
[29] K. Hu, J. Yuan, Improved robust H_∞ filtering for uncertain discrete-time switched systems, IET Control Theory Appl. 3 (3) (2009) 315–324.
[30] V. Puig, J. Quevedo, T. Escobet, A. Stancu, Robust fault detection using linear interval observers, IFAC Proc. Vol. 36 (5) (2003) 579–584.
[31] S.B. Chabane, C.S. Maniu, T. Alamo, E.F. Camacho, D. Dumur, Improved set-membership estimation approach based on zonotopes and ellipsoids, in: 2014 European Control Conference (ECC), IEEE, 2014, pp. 993–998.
[32] T. Raïssi, G. Videau, A. Zolghadri, Interval observer design for consistency checks of nonlinear continuous-time systems, Automatica 46 (3) (2010) 518–527.
[33] S. Varrier, D. Koenig, J.J. Martinez, Robust fault detection for uncertain unknown inputs LPV system, Control Eng. Pract. 22 (2014) 125–134.
[34] F. Nejjari, V. Puig, S.M. de Oca, A. Sadeghzadeh, Robust fault detection for LPV systems using interval observers and zonotopes, in: Decision and Control, 2009 held jointly with the 2009 28th Chinese Control Conference. CDC/CCC 2009. Proceedings of the 48th IEEE Conference on, IEEE, 2009, pp. 1002–1007.
[35] T. Alamo, J.M. Bravo, E.F. Camacho, Guaranteed state estimation by zonotopes, Automatica 41 (6) (2005) 1035–1043.
[36] F. Schweppe, Recursive state estimation: unknown but bounded errors and system inputs, IEEE Trans. Automat. Control 13 (1) (1968) 22–28.
[37] H. Witsenhausen, Sets of possible states of linear systems given perturbed observations, IEEE Trans. Automat. Control 13 (5) (1968) 556–558.
[38] C. Durieu, E. Walter, B. Polyak, Multi-input multi-output ellipsoidal state bounding, J. Optim. Theory Appl. 111 (2) (2001) 273–303.
[39] D. Maksarov, J. Norton, State bounding with ellipsoidal set description of the uncertainty, Int. J. Control 65 (5) (1996) 847–866.
[40] Y. Liu, Y. Zhao, F. Wu, Ellipsoidal state-bounding-based set-membership estimation for linear system with unknown-but-bounded disturbances, IET Control Theory Appl. 10 (4) (2016) 431–442.
[41] L. Chisci, A. Garulli, G. Zappa, Recursive state bounding by parallelotopes, Automatica 32 (7) (1996) 1049–1055.
[42] C. Combastel, Stable interval observers in BBC for linear systems with time-varying input bounds, IEEE Trans. Automat. Control 58 (2) (2012) 481–487.
[43] V.T.H. Le, T. Alamo, E.F. Camacho, C. Stoica, D. Dumur, Zonotopic set-membership estimation for interval dynamic systems, in: American Control Conference (ACC), 2012, IEEE, 2012, pp. 6787–6792.
[44] V.T.H. Le, C. Stoica, T. Alamo, E.F. Camacho, D. Dumur, Zonotopes: From Guaranteed State-Estimation to Control, John Wiley & Sons, 2013.
[45] J.-L. Gouzé, A. Rapaport, M.Z. Hadj-Sadok, Interval observers for uncertain biological systems, Ecol Modell 133 (1) (2000) 45–56.
[46] D. Efimov, W. Perruquetti, J.-P. Richard, On reduced-order interval observers for time-delay systems, in: 2013 European Control Conference (ECC), IEEE, 2013, pp. 2116–2121.
[47] S. Ifqir, V. Puig, D. Ichalal, N. Ait-Oufroukh, S. Mammar, Zonotopic set-membership estimation for switched systems based on wi-radius minimization: vehicle application, IFAC-PapersOnLine 53 (2) (2020) 7446–7451.
[48] Z. Fei, L. Yang, X.-M. Sun, S. Ren, Zonotopic set-membership state estimation for switched systems with restricted switching, IEEE Trans. Autom. Control (2021).
[49] V.T.H. Le, C. Stoica, T. Alamo, E.F. Camacho, D. Dumur, Zonotopic guaranteed state estimation for uncertain systems, Automatica 49 (11) (2013) 3418–3424.
[50] Y.-E. Wang, H.R. Karimi, D. Wu, Construction of hybrid interval observers for switched linear systems, Inf. Sci. 454 (2018) 242–254.
[51] C. Combastel, Zonotopes and Kalman observers: gain optimality under distinct uncertainty paradigms and robust convergence, Automatica 55 (2015) 265–273.
[52] X. Yang, J.K. Scott, A comparison of zonotope order reduction techniques, Automatica 95 (2018) 378–384.

[53] R.E. Kalman, A new approach to linear filtering and prediction problems, J. Eng. 82 (1) (1960) 35–45.
[54] M. Pourasghar, V. Puig, C. Ocampo-Martinez, Comparison of set-membership and interval observer approaches for state estimation of uncertain systems, in: 2016 European Control Conference (ECC), IEEE, 2016, pp. 1111–1116.
[55] R. Rajamani, Vehicle Dynamics and Control, Springer Science & Business Media, 2011.
[56] Q. Cheng, A.C. Victorino, A. Charara, Nonlinear observer of sideslip angle using a particle filter estimation methodology, IFAC Proc. Vol. 44 (1) (2011) 6266–6271.
[57] V. Judalet, S. Glaser, B. Lusetti, Incentive shared trajectory control for highly-automated driving, in: 2013 IEEE Intelligent Vehicles Symposium (IV), IEEE, 2013, pp. 1089–1094.